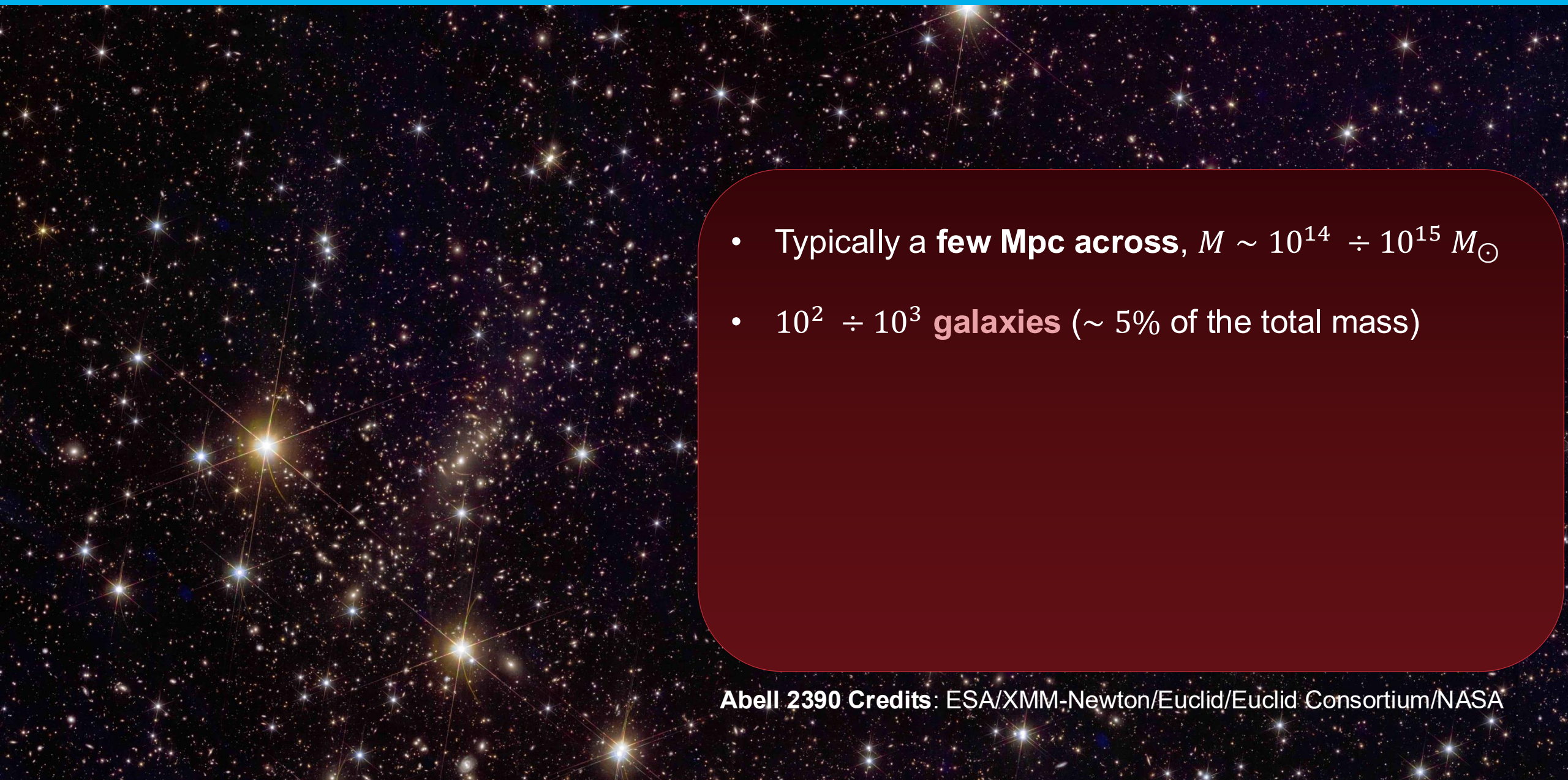
Lorenzo Pizzuti
Dipartimento di Fisica G. Occhialini – Università degli Studi Milano Bicocca



A bright era for cluster kinematics

Mass profiles from member galaxies to cosmology

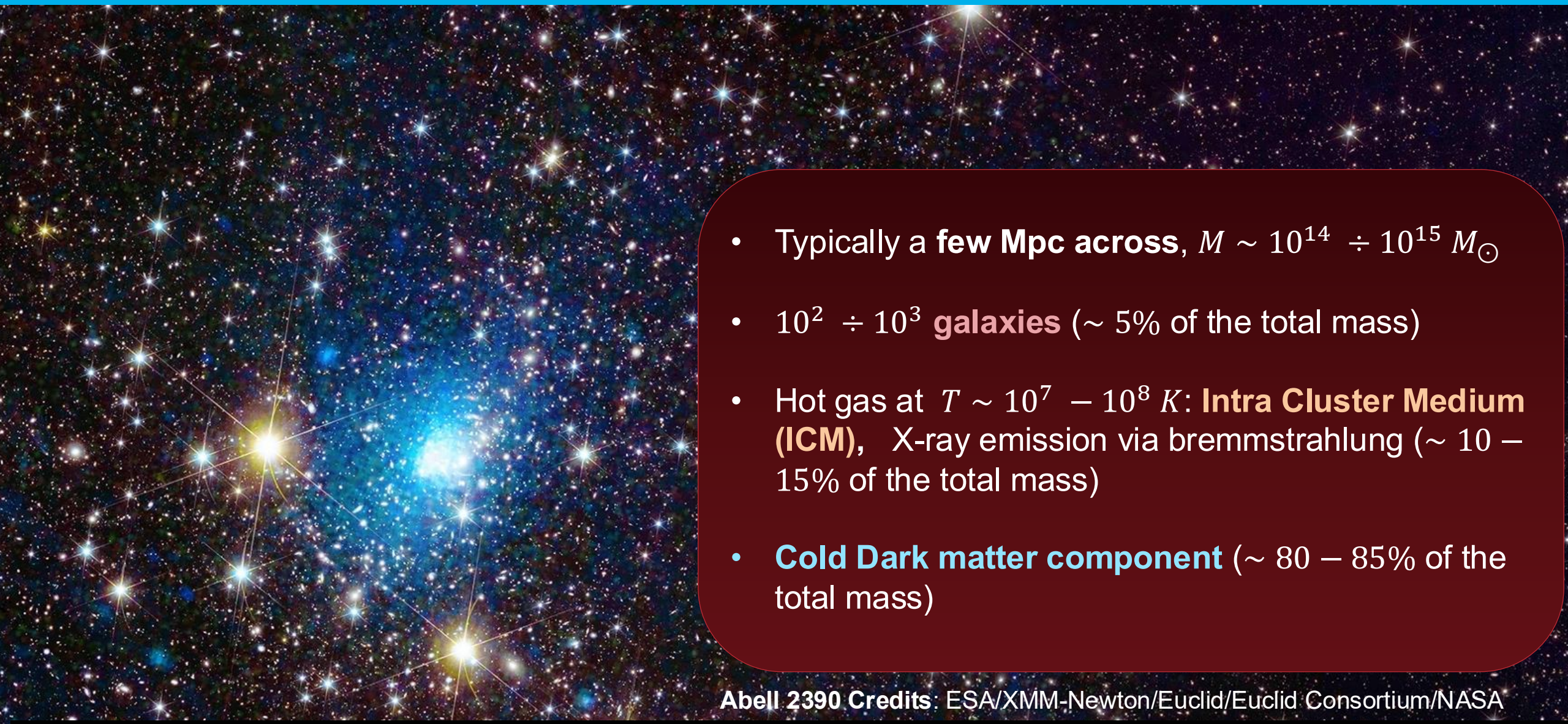
Anatomy of a galaxy cluster



- Typically a **few Mpc across**, $M \sim 10^{14} \div 10^{15}\ M_{\odot}$
- $10^{2} \div 10^{3}$ **galaxies** ($\sim 5\%$ of the total mass)

Abell 2390 Credits: ESA/XMM-Newton/Euclid/Euclid Consortium/NASA

Anatomy of a galaxy cluster

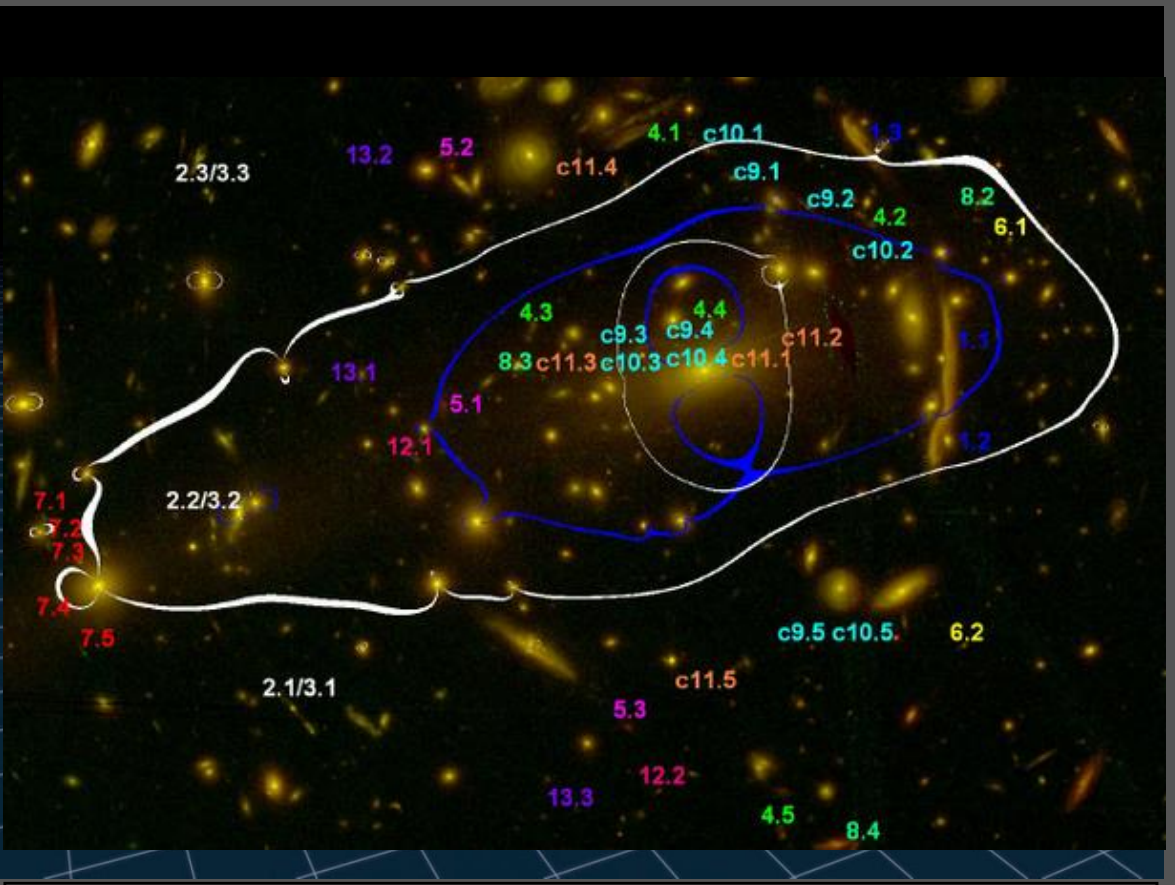


- Typically a **few Mpc across**, $M \sim 10^{14} \div 10^{15}\ M_{\odot}$
- $10^{2} \div 10^{3}$ **galaxies** ($\sim 5\%$ of the total mass)
- Hot gas at $T \sim 10^{7} - 10^{8}\ K$: **Intra Cluster Medium (ICM)**, X-ray emission via bremmstrahlung ($\sim 10 - 15\%$ of the total mass)
- **Cold Dark matter component** ($\sim 80 - 85\%$ of the total mass)

Abell 2390 Credits: ESA/XMM-Newton/Euclid/Euclid Consortium/NASA

Excellent natural laboratories between cosmology and astrophysics

Galaxy cluster mass profiles: lensing



High-quality imaging and photometric data required

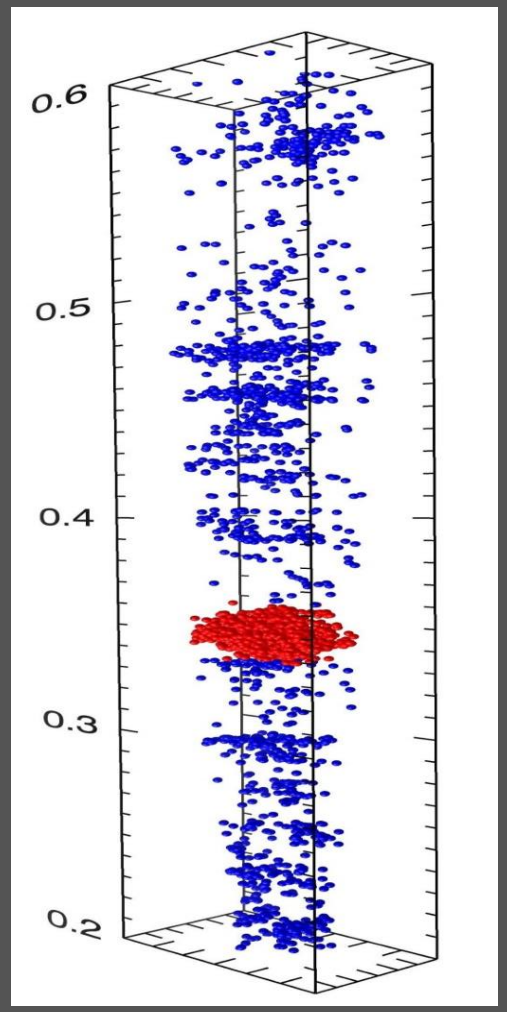
Light deflected by **gravitational potential** → estimation of mass by distortion of background sources

Strong lensing analysis: projected mass profile in the inner cluster region

Weak lensing analysis: projected mass profile in the outer cluster region

Assumptions in de-projection to recover the 3D mass

Galaxy cluster mass profiles: kinematics

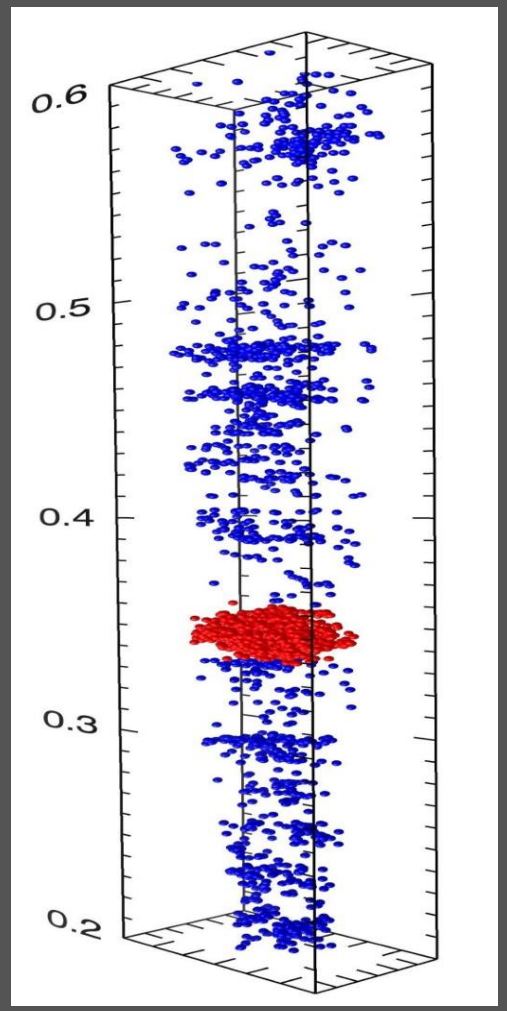


Member galaxies of the cluster RXJ 2248 (red points)

Spherical Jeans' equation:

$$\frac{d}{dr}\left[\boldsymbol{\nu(r)}\sigma_r^2\right] + 2\boldsymbol{\beta(r)}\frac{\nu(r)\sigma_r^2}{r} = -\nu(r)\frac{\boldsymbol{d\Phi}}{\boldsymbol{dr}}$$

Galaxy cluster mass profiles: kinematics



Member galaxies of the cluster RXJ 2248 (red points)

Spherical Jeans' equation:

$$\frac{d}{dr}\left[\boldsymbol{\nu(r)}\sigma_r^2\right] + 2\boldsymbol{\beta(r)}\frac{\nu(r)\sigma_r^2}{r} = -\nu(r)\frac{\boldsymbol{d\Phi}}{\boldsymbol{dr}}$$

$\boldsymbol{\nu(r)} \rightarrow$ **number density** profile of the tracers

$\boldsymbol{\sigma_r^2(r)} \rightarrow$ **velocity dispersion** along the radial direction

$\boldsymbol{\beta(r) = 1 - (\sigma_\phi^2 + \sigma_\theta^2)/2\sigma_r^2} \rightarrow$ **velocity anisotropy** profile

$$\frac{d\Phi}{dr} = \frac{GM(r)}{r^2} \rightarrow \textbf{gravitational potential}$$

Needed velocities: spectroscopic redshift data required

Assumption of **dynamical relaxation** and **spherical symmetry**

Galaxy cluster mass profiles: kinematics

Historically, **the first indication of a dark matter** component in clusters comes from the motion of the member galaxies



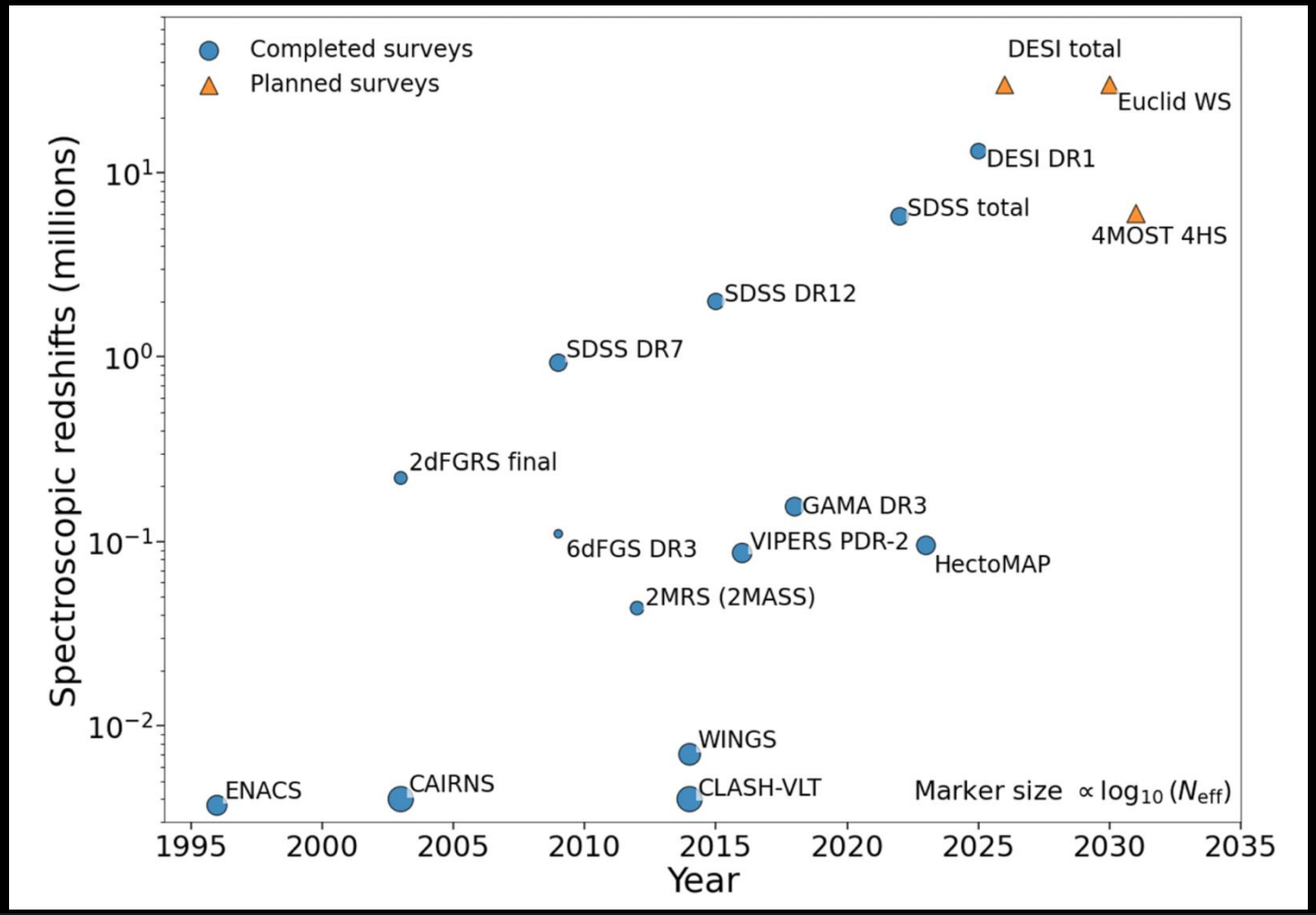
Gravitating mass of the Coma cluster obtained by F. Zwicky (1933, 1937)

$$\frac{M}{L} \sim 300 - 500 \frac{M_\odot}{L_\odot}$$

Estimated using the **virial theorem**

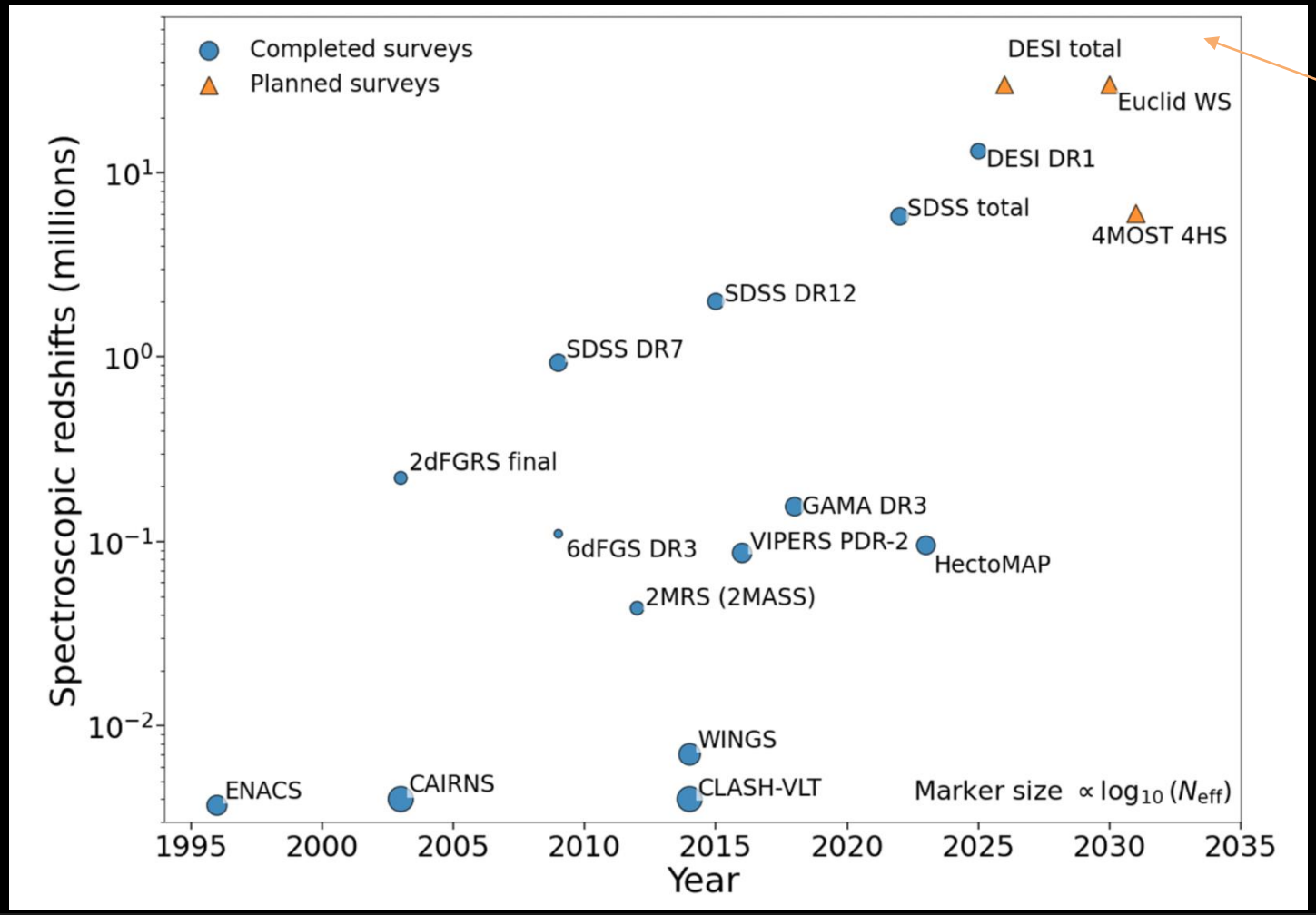
$$M \sim \frac{3\sigma_{los}^2 R}{G}$$

For decades, kinematics of clusters limited by the **number of spectroscopic redshifts** for the member galaxies
In the recent years: **new facilities and new techniques → sophisticated and reliable** mass profile measurements.



From Biviano Pizzuti, Diaferio, 2026, A&A Rev., 34, 9.
Size proportional to the logarithm of the number of galaxies per cluster

For decades, kinematics of clusters limited by the **number of spectroscopic redshifts** for the member galaxies
In the recent years: **new facilities and new techniques** → **sophisticated and reliable** mass profile measurements.



Large datasets, high resolution

Example: **WST** $\sim 2\times10^8$ redshifts with expected error of $\sim 10\ \mathrm{km/s}$

Higher redshift $z \gtrsim 1$ where other probes become less informative

Novel methods:

Full phase space information (Jeans-based methods, caustics)
Advance Machine Learning techniques
Multi probe analyses!

From Biviano Pizzuti, Diaferio, 2026, A&A Rev., 34, 9.
Size proportional to the logarithm of the number of galaxies per cluster

Galaxy cluster mass profiles: dynamics vs lensing analysis

Spacetime of a galaxy cluster**: linear perturbation** of FRW metric

$$\boldsymbol{ds^2 = a^2(\tau)\left[-\left(1+\frac{2\Phi}{c^2}\right)c^2 d\tau^2 + \left(1-\frac{2\Psi}{c^2}\right)dl^2\right]},$$

$\Phi, \Psi \sim 10^{-4}c^2$ gravitational potentials

In standard GR: $\Phi = \Psi \equiv \Phi_N$

$\Phi \neq \Psi \rightarrow$ Signatures of modified gravity

Galaxy cluster mass profiles: dynamics vs lensing analysis

Spacetime of a galaxy cluster**: linear perturbation** of FRW metric

$$ds^2 = a^2(\tau)\left[-\left(1+\frac{2\Phi}{c^2}\right)c^2 d\tau^2 + \left(1-\frac{2\Psi}{c^2}\right)dl^2\right], \quad \Phi, \Psi \sim 10^{-4}c^2 \text{ gravitational potentials}$$

In standard GR: $\Phi = \Psi \equiv \Phi_N$ $\Phi \neq \Psi \rightarrow$ Signatures of modified gravity

Constrain Φ, Ψ ⇨ Constrain deviation from General Relativity

Galaxy cluster mass profiles: dynamics vs lensing analysis

Spacetime of a galaxy cluster: **linear perturbation** of FRW metric

$$ds^2 = a^2(\tau)\left[-\left(1+\frac{2\Phi}{c^2}\right)c^2 d\tau^2 + \left(1-\frac{2\Psi}{c^2}\right)dl^2\right], \quad \Phi, \Psi \sim 10^{-4}c^2 \text{ gravitational potentials}$$

In standard GR: $\Phi = \Psi \equiv \Phi_N$ $\Phi \neq \Psi \rightarrow$ Signatures of modified gravity

Constrain Φ, Ψ ⇨ Constrain deviation from General Relativity

Motion of galaxies (kinematic analysis): **TIME-TIME Φ**

Photons (lensing analysis): **TIME-TIME** + **SPACE-SPACE** $\Phi_{lens} = \frac{1}{2}(\Phi + \Psi)$

MG-MAMPOSSt

MAMPOSSt = Modelling Anisotropy and Mass Profile of Observed Spherical System

Developed by *Mamon, Biviano, Boué* (MNRAS 429 (Mar. 2013)3079–3098)

Jeans' equation solved in the **projected phase-pace** (R, v_z)



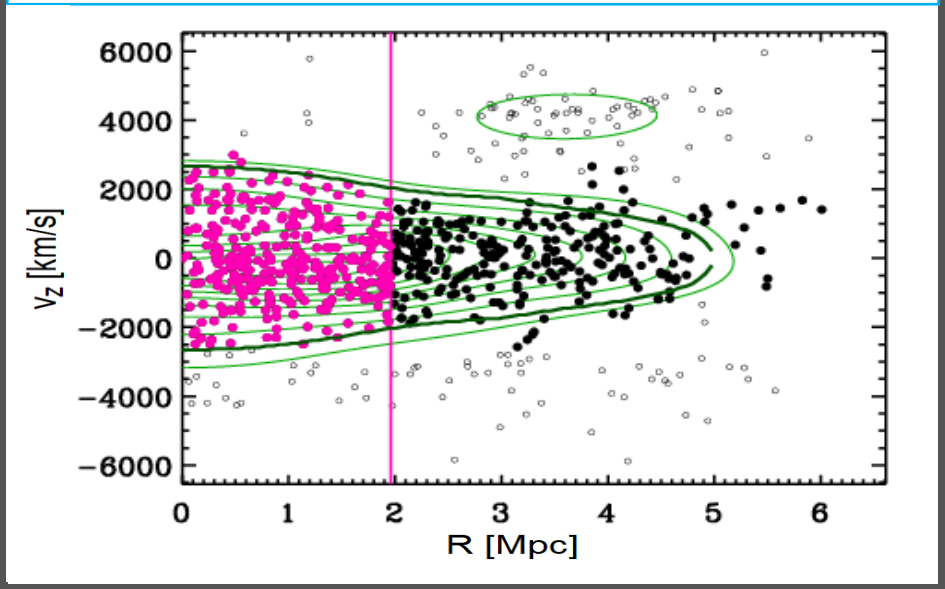
MG-MAMPOSSt

MAMPOSSt = Modelling Anisotropy and Mass Profile of Observed Spherical System

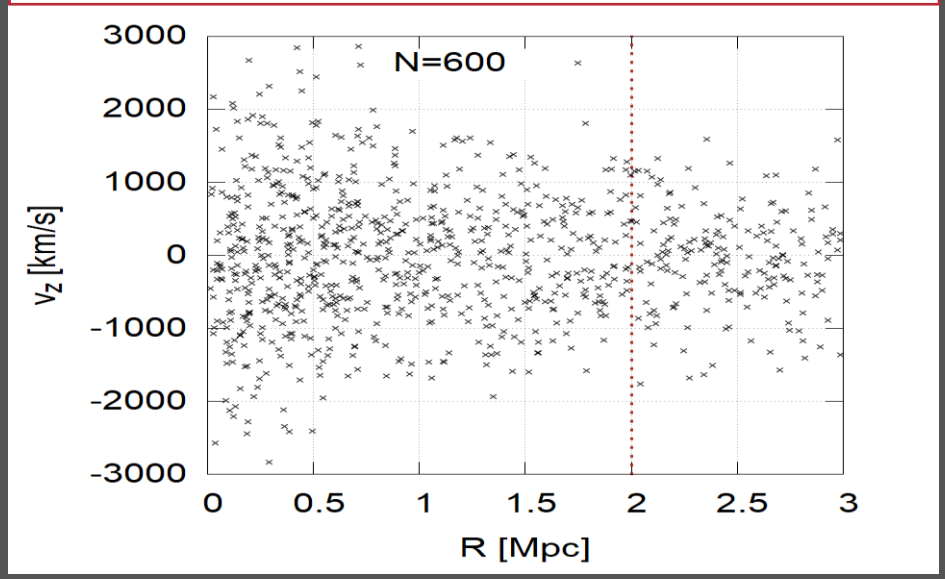
Developed by *Mamon, Biviano, Boué* (MNRAS 429 (Mar. 2013)3079–3098)

Jeans' equation solved in the **projected phase-pace** (R, v_z)

Real cluster MACS 1206 (Biviano et al., 2013)



Synthetic cluster N=600 (Pizzuti et al., 2021)



Maximum Likelihood fit to obtain the parameters of kinematics quantities

MG-MAMPOSSt (*Pizzuti L., Saltas I.D., Amendola L., 2021*)

$$\sigma_r^2(r) = \frac{1}{\nu(r)} \int_r^\infty ds \exp\left[2 \int_r^s \frac{\beta(t)}{t} dt\right] \nu(s) \frac{d\Phi}{ds}$$

$\beta(r) \rightarrow$ anisotropy profile

$\nu(r) \rightarrow$ number density profile

Parameter space: GR

MG-MAMPOSSt:

- **Modified Newtonian potential**
- **Chameleon** screening, **Vainshtein** screening (DHOST), Refracted Gravity, Clustering DE
- **Grid /MCMC** (Metropolis-Hastings) parameter space exploration.
- Modules to include additional information (e.g. lensing, X-ray posteriors) for joint analyses
- **Generalised anisotropy and BCG dynamics**

MG-MAMPOSSt (*Pizzuti L., Saltas I.D., Amendola L., 2021*)

$$\sigma_r^2(r) = \frac{1}{\nu(r)} \int_r^\infty ds \exp\left[2 \int_r^s \frac{\beta(t)}{t} dt\right] \nu(s) \frac{d\Phi}{ds}$$

$\beta(r) \rightarrow$ anisotropy profile

$\nu(r) \rightarrow$ number density profile

Parameter space: GR + non-standard params: $\mathcal{M}_1, \mathcal{M}_2, \mathcal{M}_3$

$$\mathcal{M}_i = \begin{cases} Y_1, Y_2 & VS \\ Q, \phi_\infty & CS \\ \epsilon_0, \rho_c, Q & RG \\ f_{DE}\ c_s^2 & CDE \end{cases}$$

MG-MAMPOSSt:

- **Modified Newtonian potential**
- **Chameleon** screening, **Vainshtein** screening (DHOST), Refracted Gravity, Clustering DE
- **Grid /MCMC** (Metropolis-Hastings) parameter space exploration.
- Modules to include additional information (e.g. lensing, X-ray posteriors) for joint analyses
- **Generalised anisotropy and BCG dynamics**

An overview of what we can do…

MG - MAMPOSSt

An overview of what we can do…

- Lensing + kinematics (+X-ray?)
- Test idealised scenarios (simulations) to explore new models

Constrain MG and DE models



MG - MAMPOSSt

An overview of what we can do…

- Lensing + kinematics (+X-ray?)
- Test idealised scenarios (simulations) to explore new models

Constrain MG and DE models

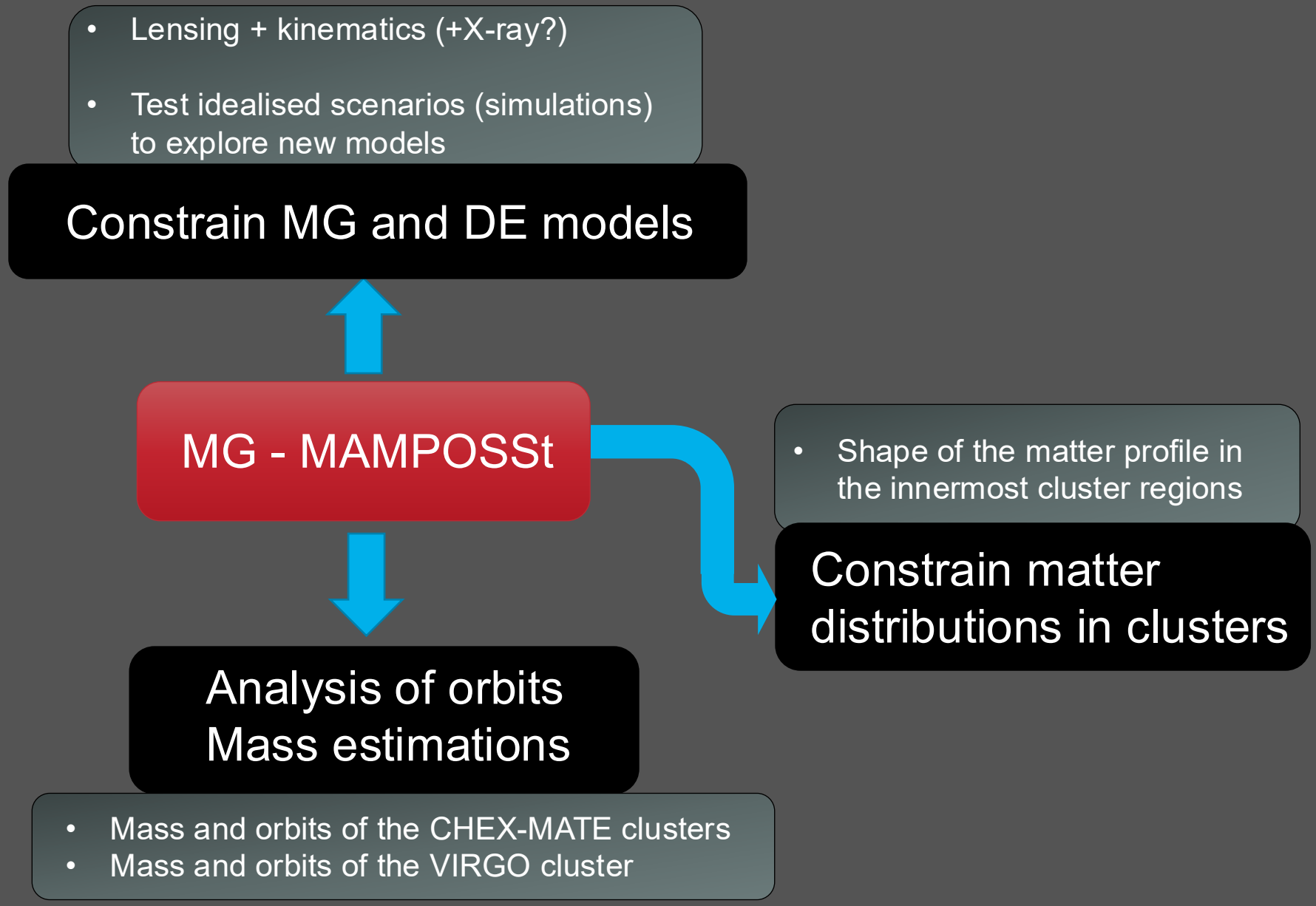


MG - MAMPOSSt

- Shape of the matter profile in the innermost cluster regions

Constrain matter distributions in clusters

An overview of what we can do…



An overview of what we can do…

- Lensing + kinematics (+X-ray?)
- Test idealised scenarios (simulations) to explore new models

Constrain MG and DE models

MG - MAMPOSSt

- Shape of the matter profile in the innermost cluster regions

Constrain matter distributions in clusters

Constrain alterantives to dark matter

- Refracted Gravity
- Boson stars and solitonic objects
- MOND-like models

Analysis of orbits Mass estimations

- Mass and orbits of the CHEX-MATE clusters
- Mass and orbits of the Coma and Virgo clusters

Data from **CLASH** and **CLASH-VLT** collaborations

MACSJ-1206



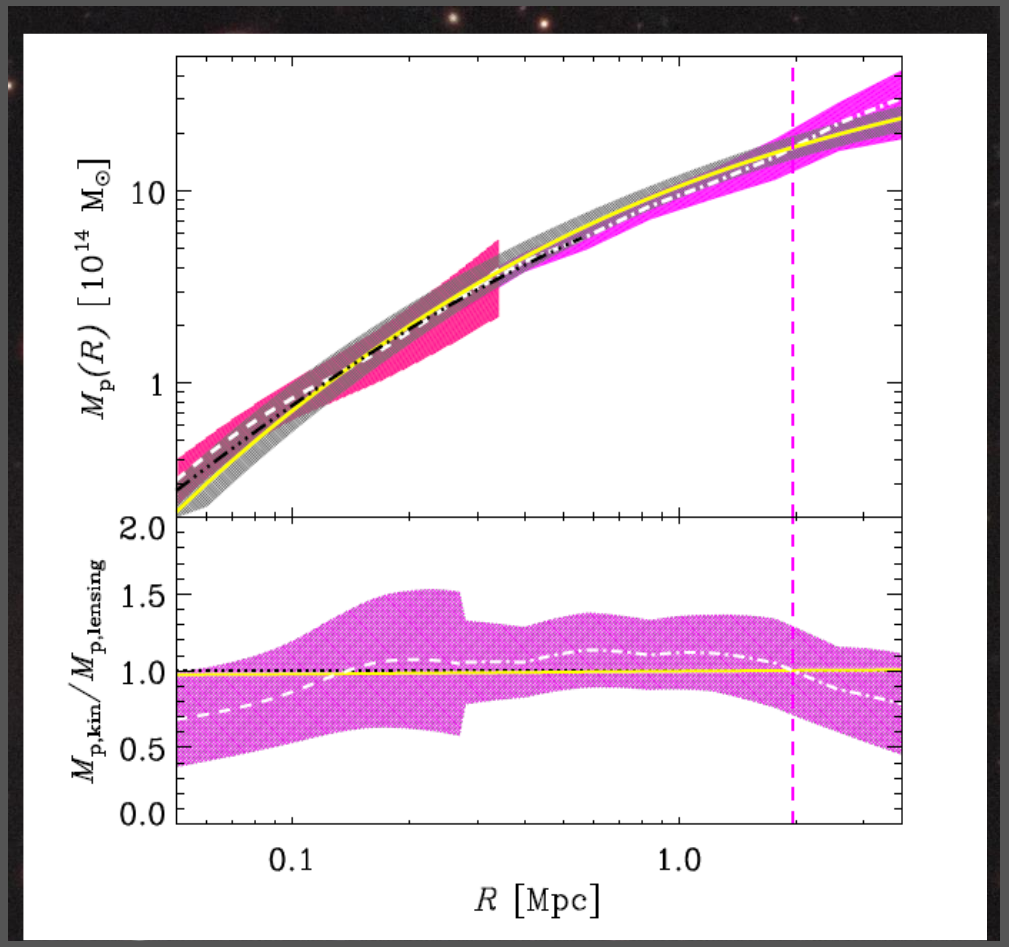
- Subaru+HST
- VLT/VIMOS + MUSE

Abell S1063



Data from **CLASH** and **CLASH-VLT** collaborations

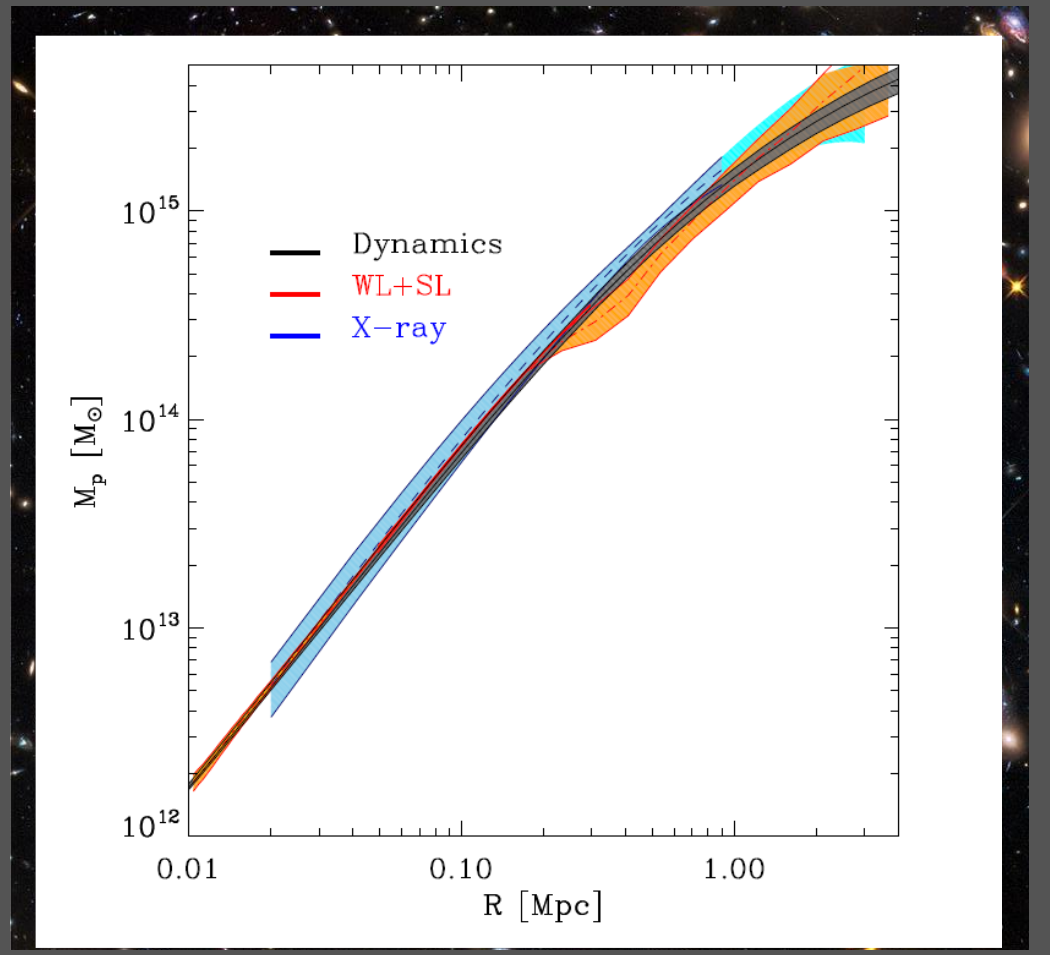
MACSJ-1206



Credits: Biviano et al., 2013

- Subaru+HST
- VLT/VIMOS + MUSE

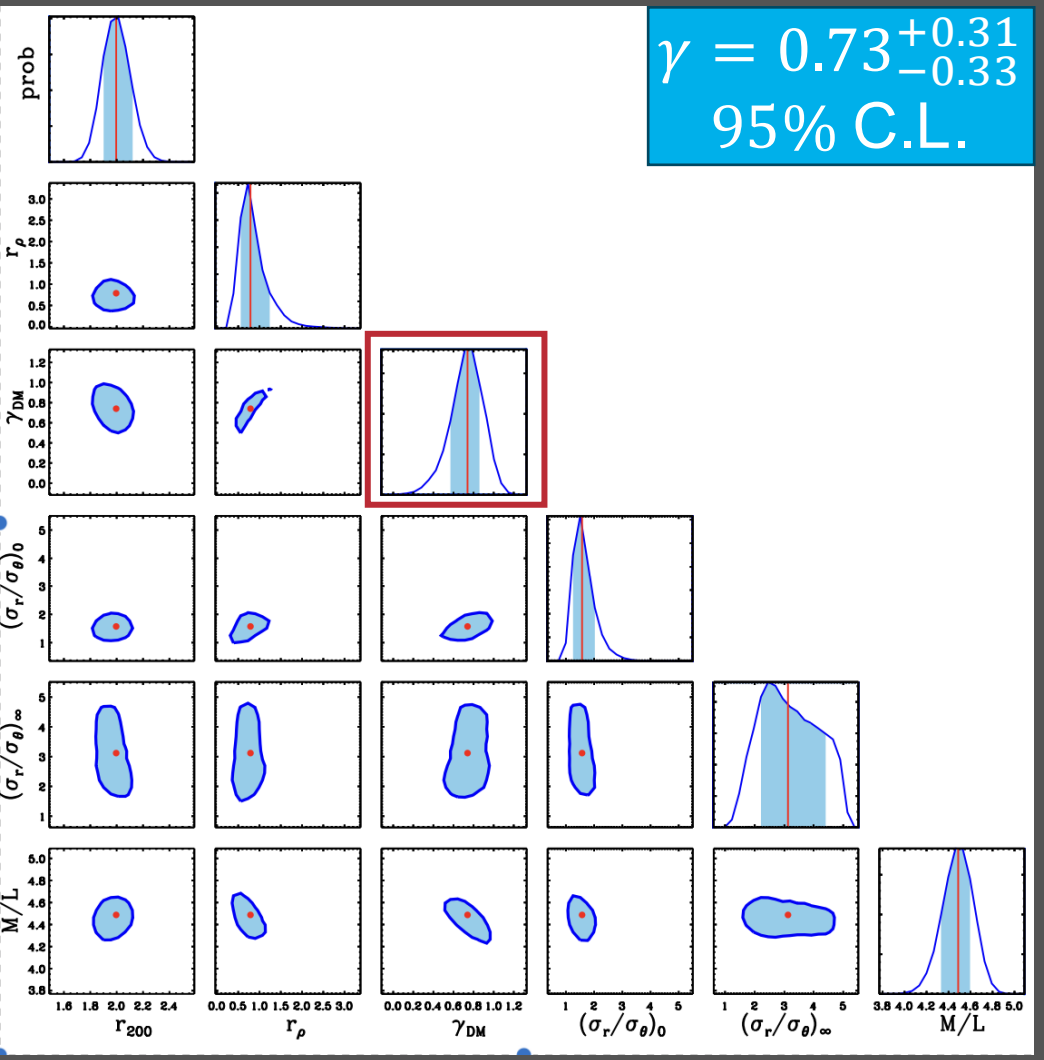
Abell S1063



Credits: Sartoris et al., 2020

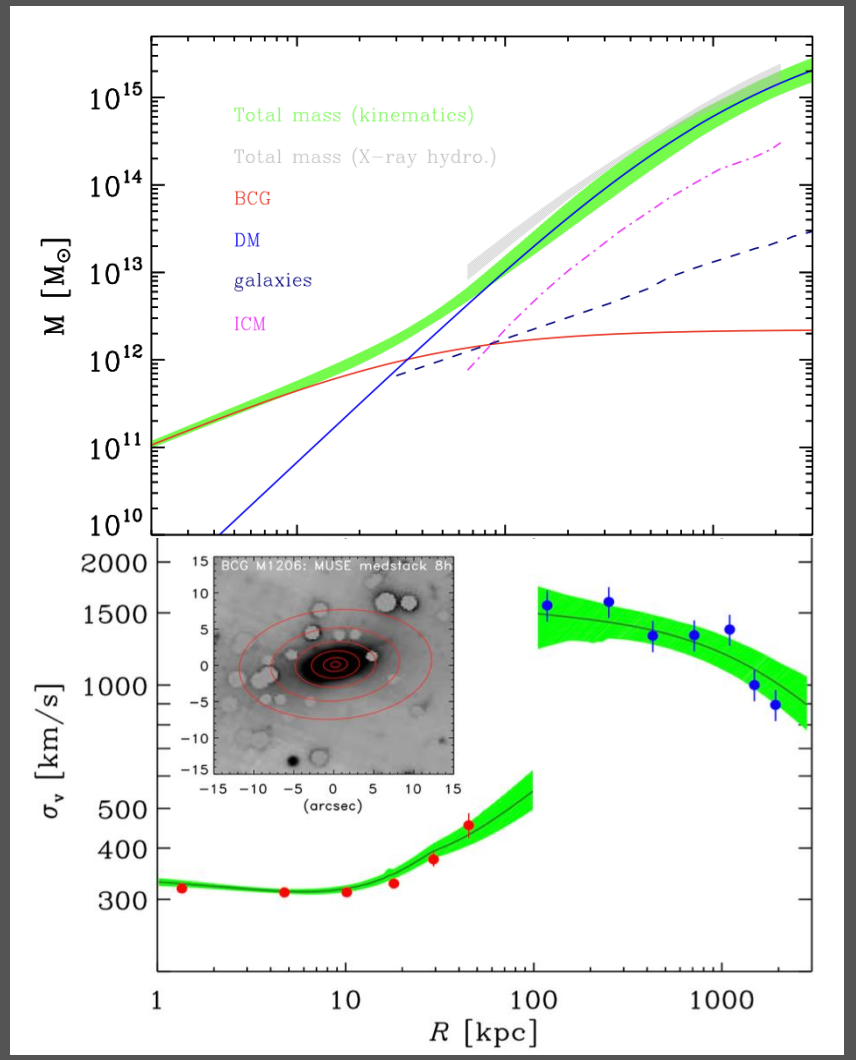
What if we further have the velocity dispersion of the BCG?

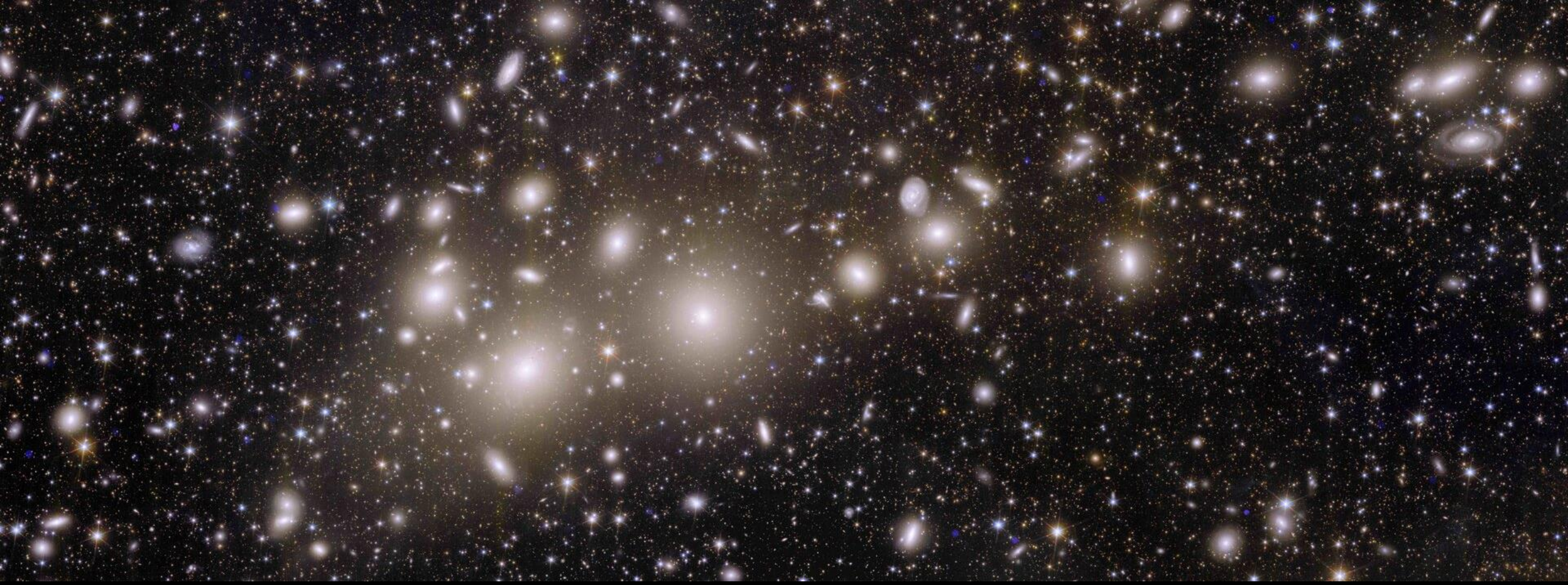
A. Biviano, **LP,** et al., 2023 [10.3847/1538-4357/acf832](https://doi.org/10.3847/1538-4357/acf832)



$$\gamma = 0.73^{+0.31}_{-0.33}$$
95% C.L.

$$\rho_{gNFW}(r) = \frac{\rho_s}{\left(\frac{r}{r_s}\right)^{\gamma}\left(1+\frac{r}{r_s}\right)^{3-\gamma}}$$





Refracted Gravity

REFRACTED GRAVITY

The MG-MAMPOSSt+BCG method can be applied to test alternatives to Dark Matter

Refracted gravity (RG) model (Matsakos & Diaferio, 2016): modified Poisson eq. **with a gravitational permittivity $\epsilon(\rho)$,** which depends on the matter density

In spherical symmetry: $$\frac{\mathrm{d}\Phi}{\mathrm{d}r} = \frac{GM(r)}{\epsilon(\rho) r^2}$$

$$\epsilon(\rho) = \epsilon_0 + (1-\epsilon_0)\frac{1}{2}\left\{\tanh\left[\ln\left(\frac{\rho}{\rho_c}\right)^Q\right] + 1\right\}$$

REFRACTED GRAVITY

The MG-MAMPOSSt+BCG method can be applied to test alternatives to Dark Matter

Refracted gravity (RG) model (Matsakos & Diaferio, 2016): modified Poisson eq. **with a gravitational permittivity $\epsilon(\rho)$,** which depends on the matter density

In spherical symmetry: $$\frac{\mathrm{d}\Phi}{\mathrm{d}r} = \frac{GM(r)}{\epsilon(\rho) r^2}$$

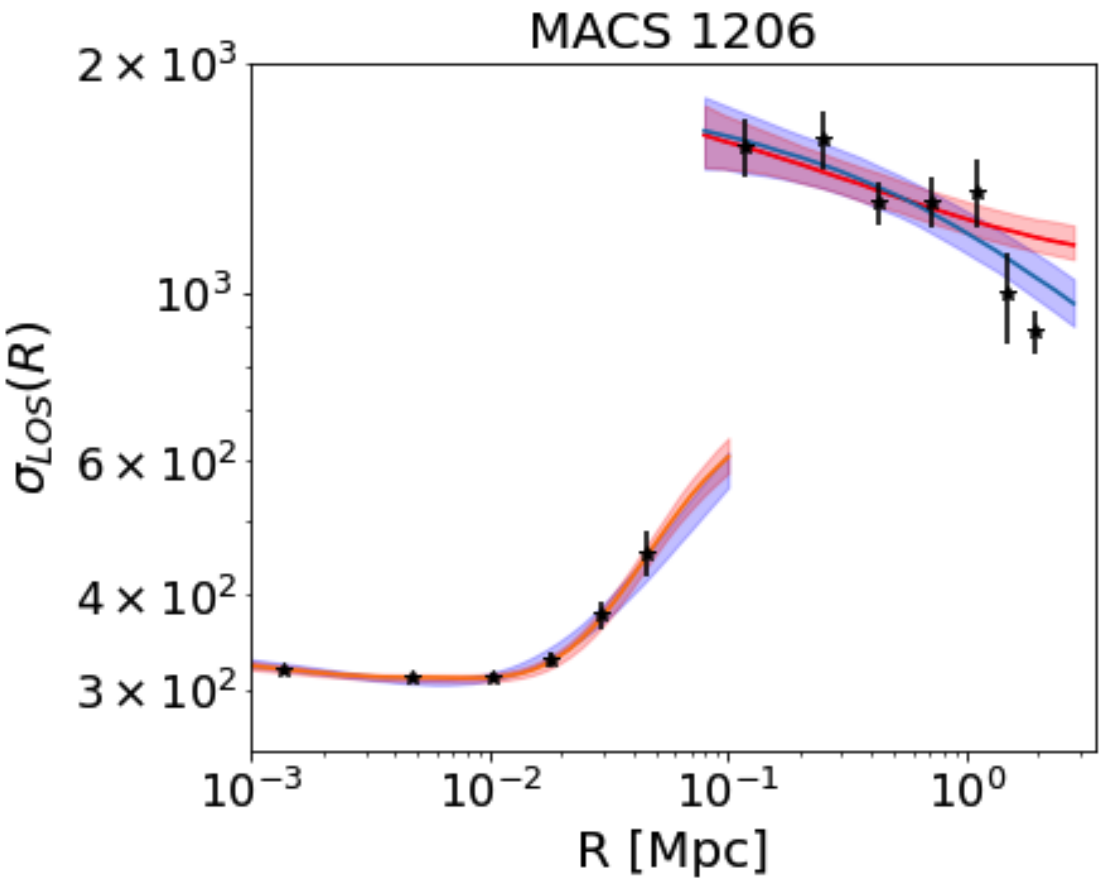
$$\epsilon(\rho) = \boldsymbol{\epsilon_0} + (1 - \boldsymbol{\epsilon_0}) \frac{1}{2} \left\{ \tanh \left[\ln \left(\frac{\rho}{\boldsymbol{\rho_c}} \right)^{\boldsymbol{Q}} \right] + 1 \right\}$$

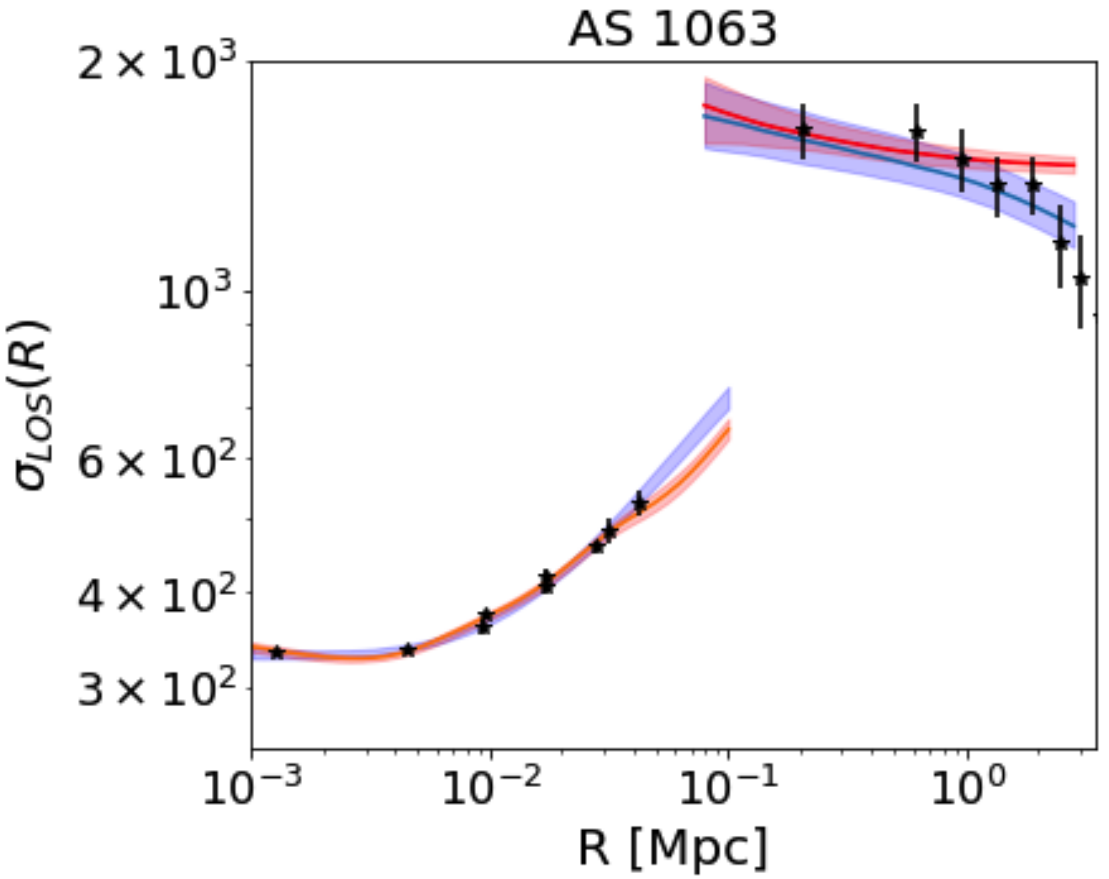
Recently, a covariant formulation has been proposed (Sanna et al., 2023), where the full Dark sector is covered by a single scalar field ϕ

Aim: test RG paradigm using data of BCG velocity dispersion and member galaxies in MACS 1206 and AS1063

$$M(r) = M_{BCG}(r) + \boxed{M_{gas}(r) + M_{gal}(r)} \rightarrow \text{OBSERVED!}$$

REFRACTED GRAVITY



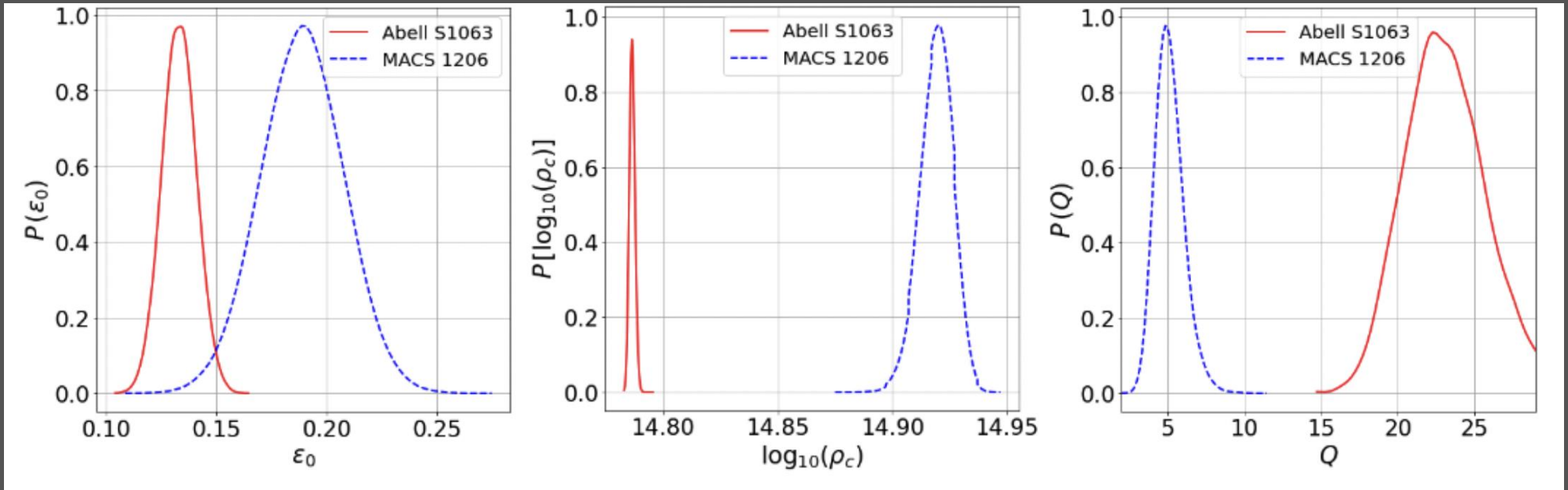


Pizzuti et al, 2025a, https://doi.org/10.1051/0004-6361/202452739

$\Delta BIC(AS1063) = 4.1$ **in favour of GR**
$\Delta BIC(MACS1206) = 2.1$ **in favour of GR**

No strong preference for GR. However, INCONSISTENT values of the free parameters between the two clusters

REFRACTED GRAVITY



parameter	Disk galaxies	Elliptical galaxies	MACS 1206	Abell S1063
$\log_{10}\left[\rho_c/(\mathrm{g}_\odot/\mathrm{cm}^3)\right]$	$-24.54^{+0.08}_{-0.07}$	$-24.25^{+0.28}_{-0.20}$	$-25.25^{+0.01}_{-0.01}$	$-25.383^{+0.003}_{-0.002}$
ϵ_0	$0.666^{+0.007}_{-0.007}$	$0.089^{+0.038}_{-0.035}$	$0.18^{+0.04}_{-0.04}$	$0.13^{+0.01}_{-0.01}$
Q	$1.79^{+0.14}_{-0.26}$	$0.47^{+0.29}_{-0.21}$	$5.21^{+1.85}_{-1.70}$	$23.62^{+5.00}_{-4.69}$

Table 3. Results comparison between the RG parameters of this work with the previous ones

REFRACTED GRAVITY: understanding systematics

~ 70% of simulated cluster population **leads to spurious detections of MG**

REFRACTED GRAVITY: understanding systematics

~ 70% of simulated cluster population **leads to spurious detections of MG**

---

2 observational criteria related to systematics DIRECTLY from the pps

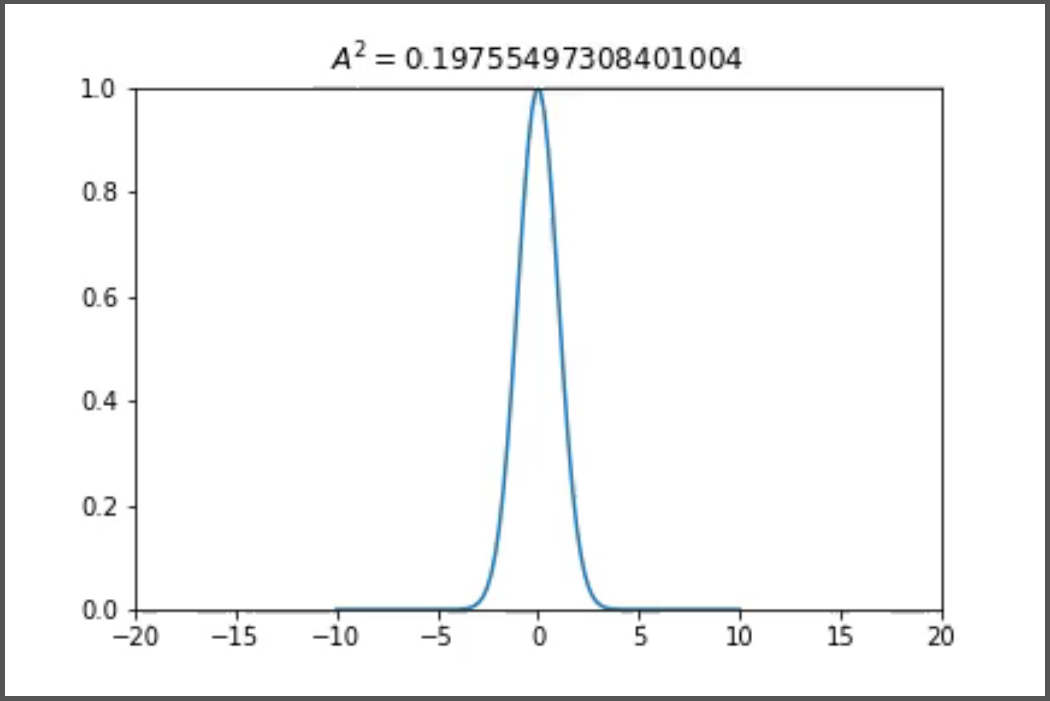
REFRACTED GRAVITY: understanding systematics

~ 70% of simulated cluster population **leads to spurious detections of MG**

---

2 observational criteria related to systematics DIRECTLY from the pps

Anderson-Darling coefficient A^2 → deviations from Gaussianity of the los velocity distribution:



SMALL A^2: more relaxed



LARGE A^2: less relaxed



REFRACTED GRAVITY: understanding systematics

~ 70% of simulated cluster population **leads to spurious detections of MG**

---

2 observational criteria related to systematics DIRECTLY from the pps

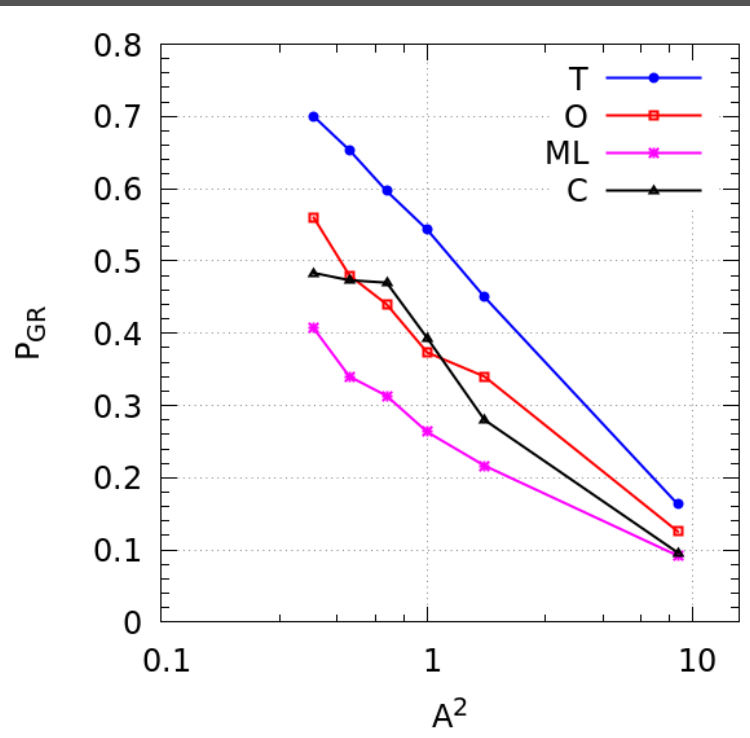
Anderson-Darling coefficient A^2 → deviations from Gaussianity of the los velocity distribution:

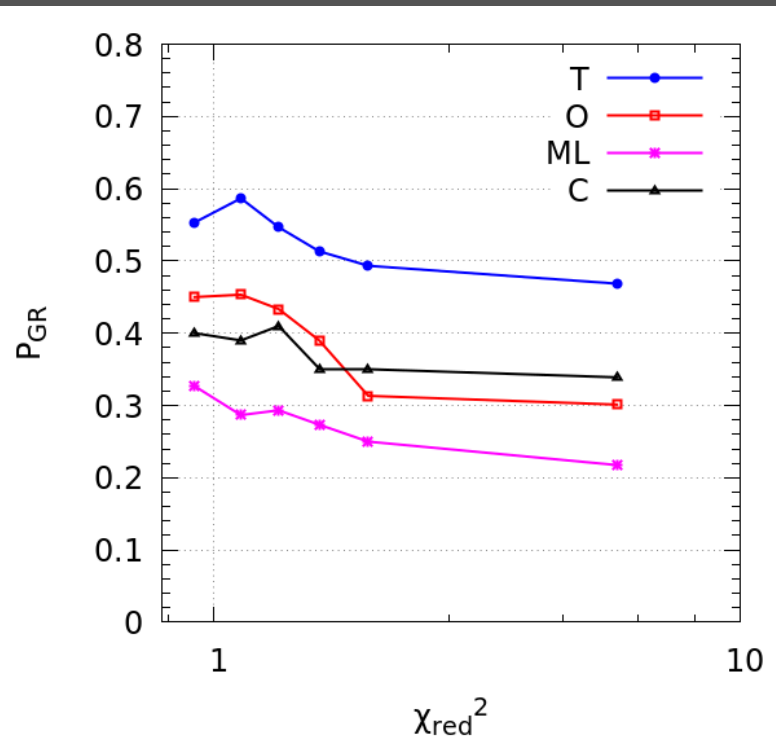
χ^2 from fitting the projected number density with a pNFW profile →

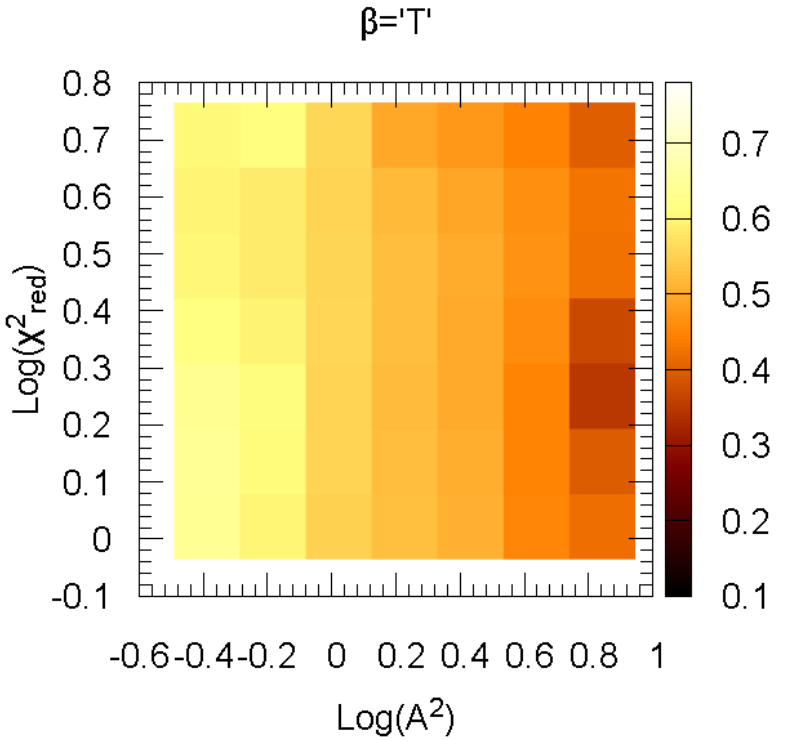
- deviations from sph. symmetry,
- parametrization of the profile,
- substructures in the pps

REFRACTED GRAVITY: understanding systematics

Systematics related to the lack of the main assumptions: **dynamical relaxation** and **sph. symmetry.** A^2, χ_ν^2 **→help in selecting suitable halos**



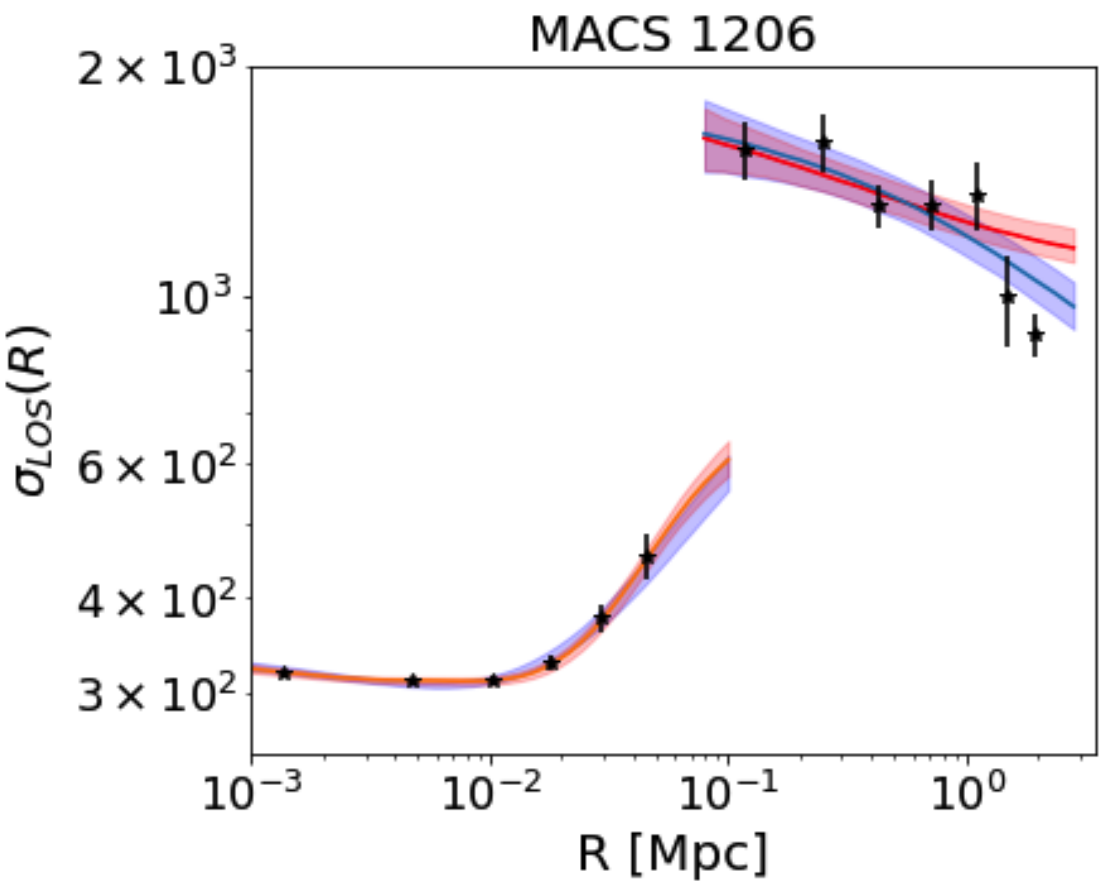


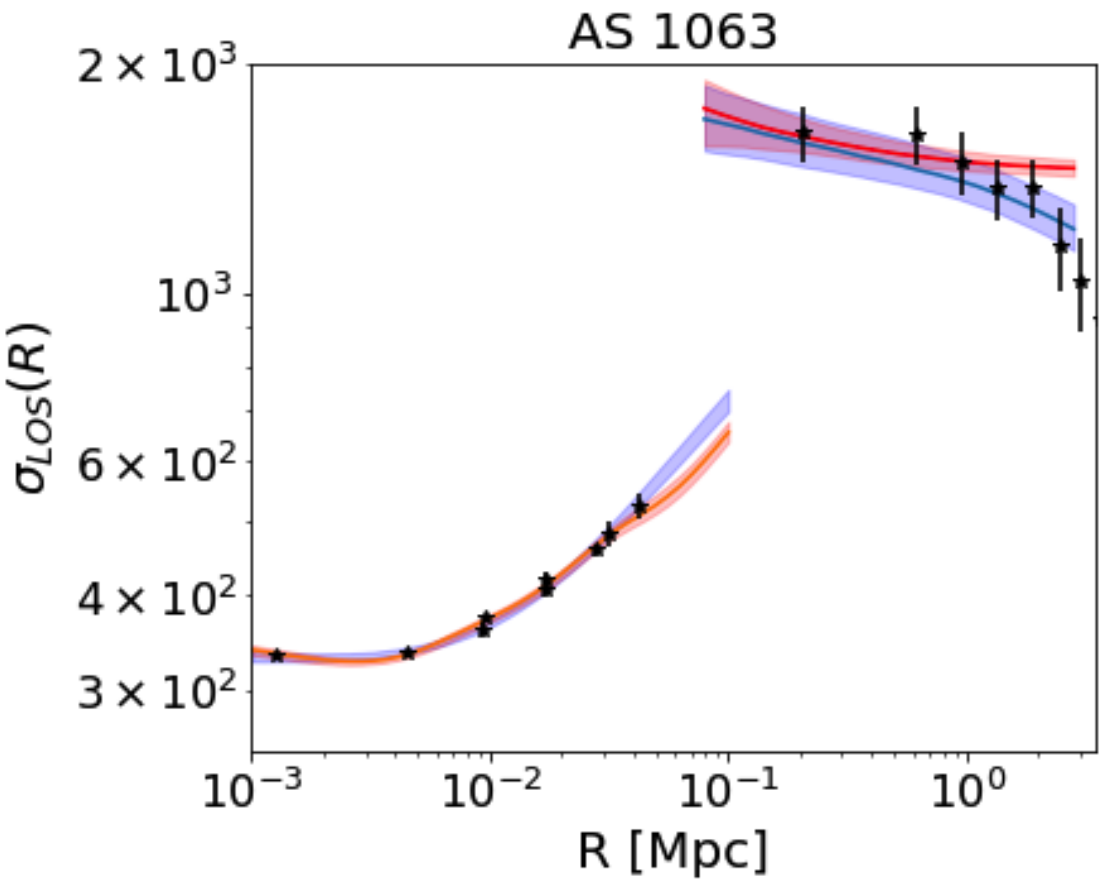


Percentage of spurious detection lowered **down to ~ 20%** for $A^2 < 1,\ \chi^2_{red} < 0.5$

TREND INDEPENDENT OF THE ANISOTROPY MODEL

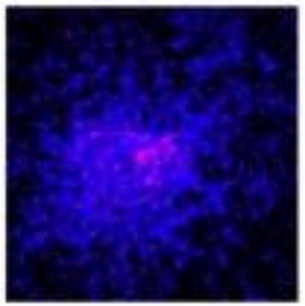
REFRACTED GRAVITY



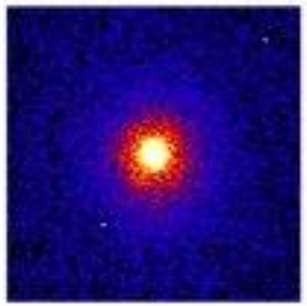


$A^2 = 0.64$

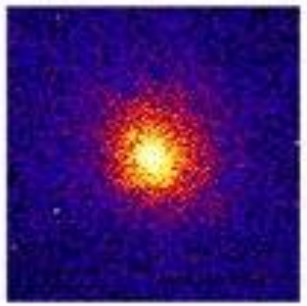
$A^2 = 1.04$



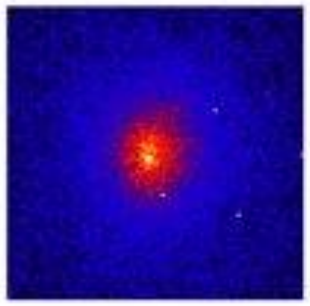
Abell 209



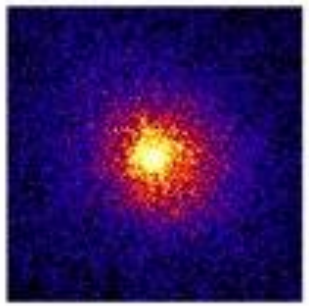
Abell 383



Abell 611



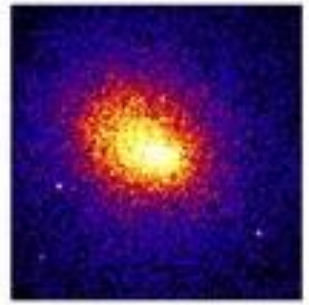
Abell 963



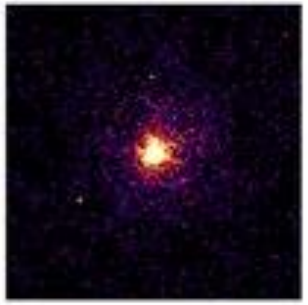
Abell 2261



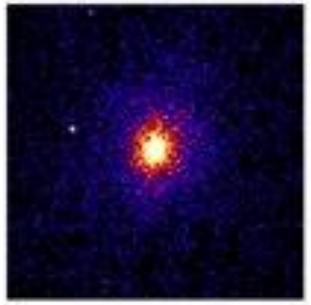
MACS 1720+3536



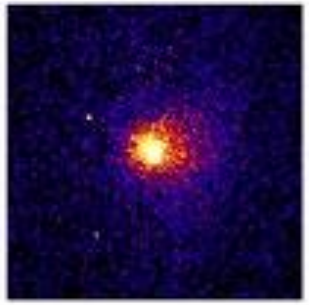
RXJ 2248-4431



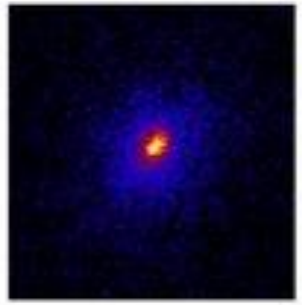
MACS 0329-0211



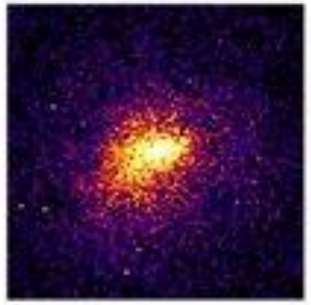
MACS 0429-0253



MACS 0744+3927



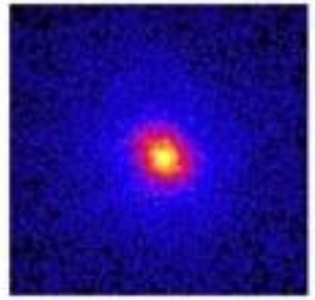
MACS 1115+0129



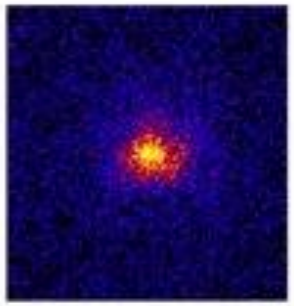
MACS 1206-0847



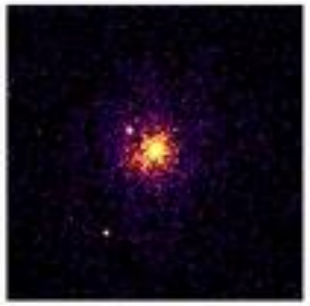
MACS 1931-2634



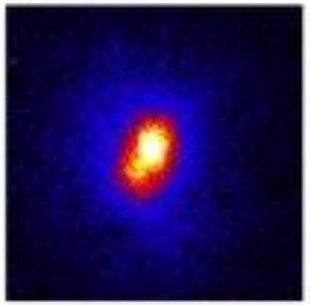
MS-2137



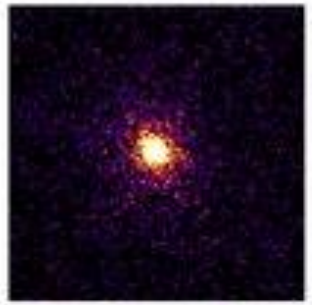
CLJ1226+3332



MACS 1311-0310



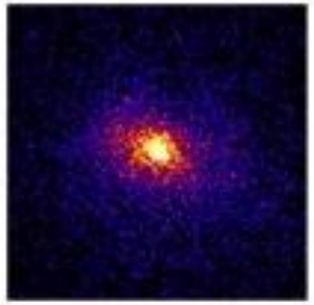
RXJ 1347-1145



MACS 1423+2404



RXJ 1532+3020



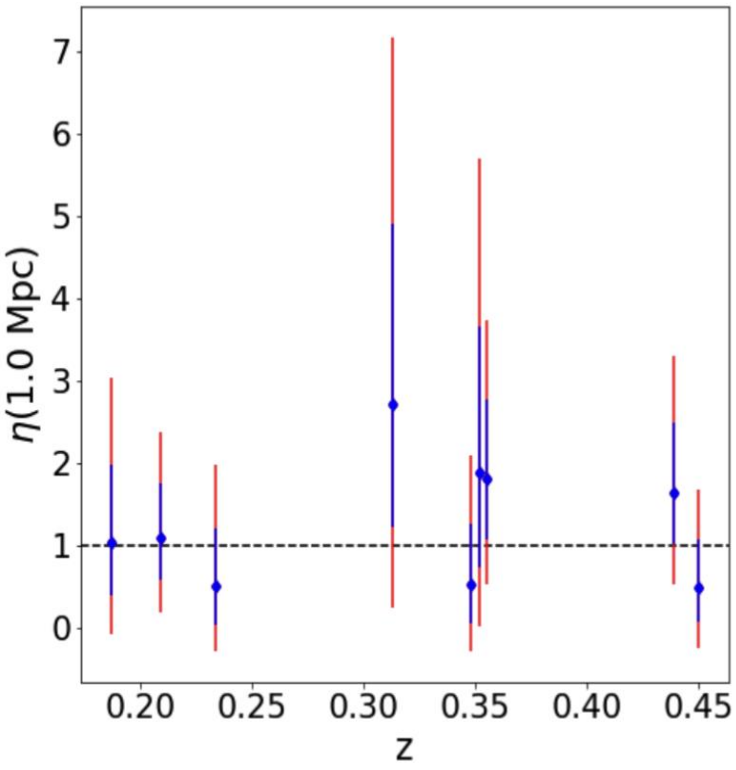
RXJ 2129+0005

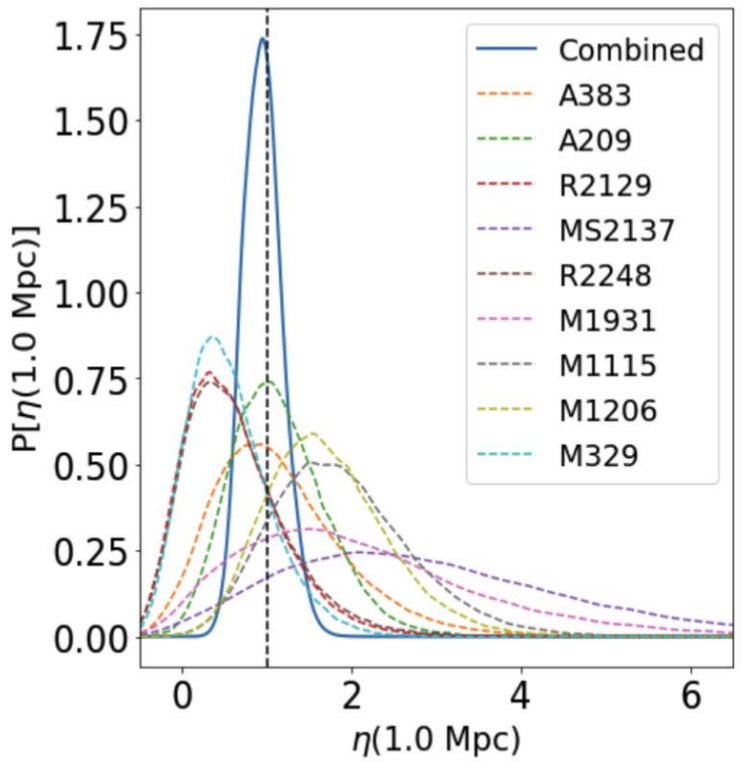


More statistics! The CLASH sample

Testing genuine departures from GR using nine CLASH clusters

Ratio between the scalar potentials of the perturbed metric of a cluster: $\eta = \frac{\Psi}{\Phi}$





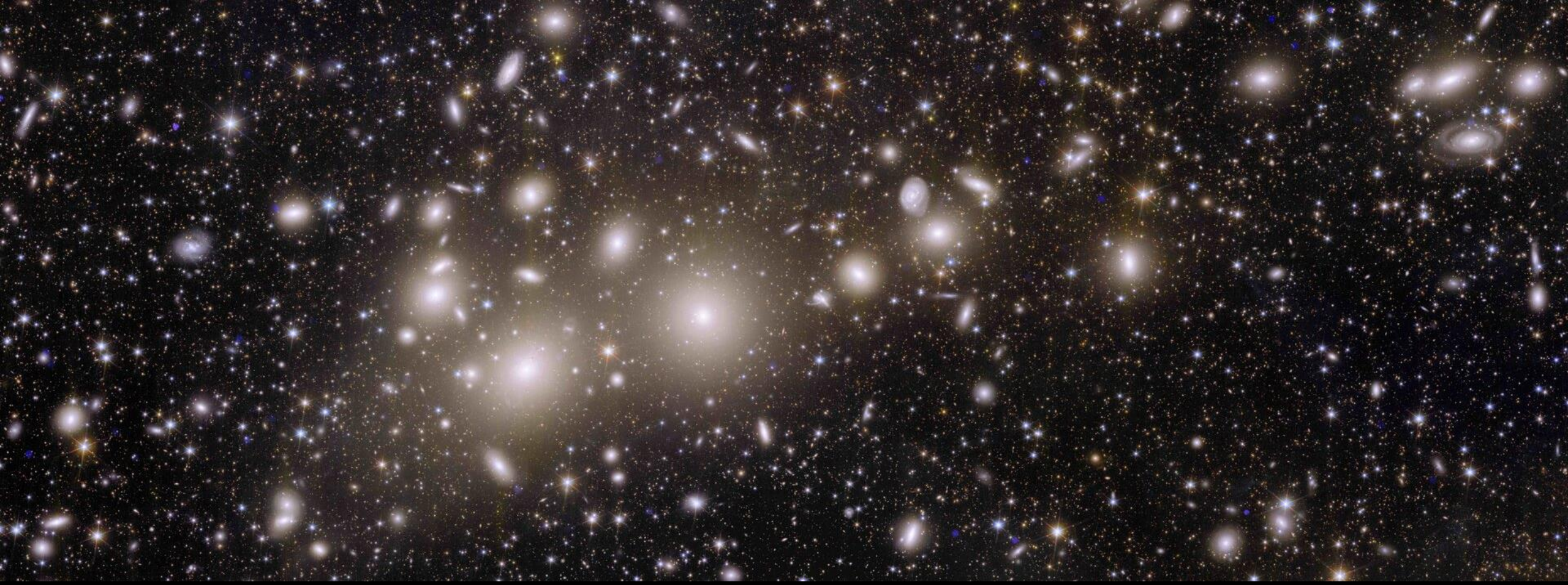
Pizzuti et al., 2026a, *JCAP* 03 (2026) 022

Combined distribution: in agreement with GR expectation ($\eta = 1$)

NFW mass profile: on average best fit for the *total* mass of each cluster.

Lensing data from Umetsu et al., 2016
Kinematics data from the CLASH-VLT team

$$\eta(r = 1\,\mathrm{Mpc}) = 0.93^{+0.48}_{-0.40}\,(stat, 2\sigma) \pm 0.47\,(syst)$$

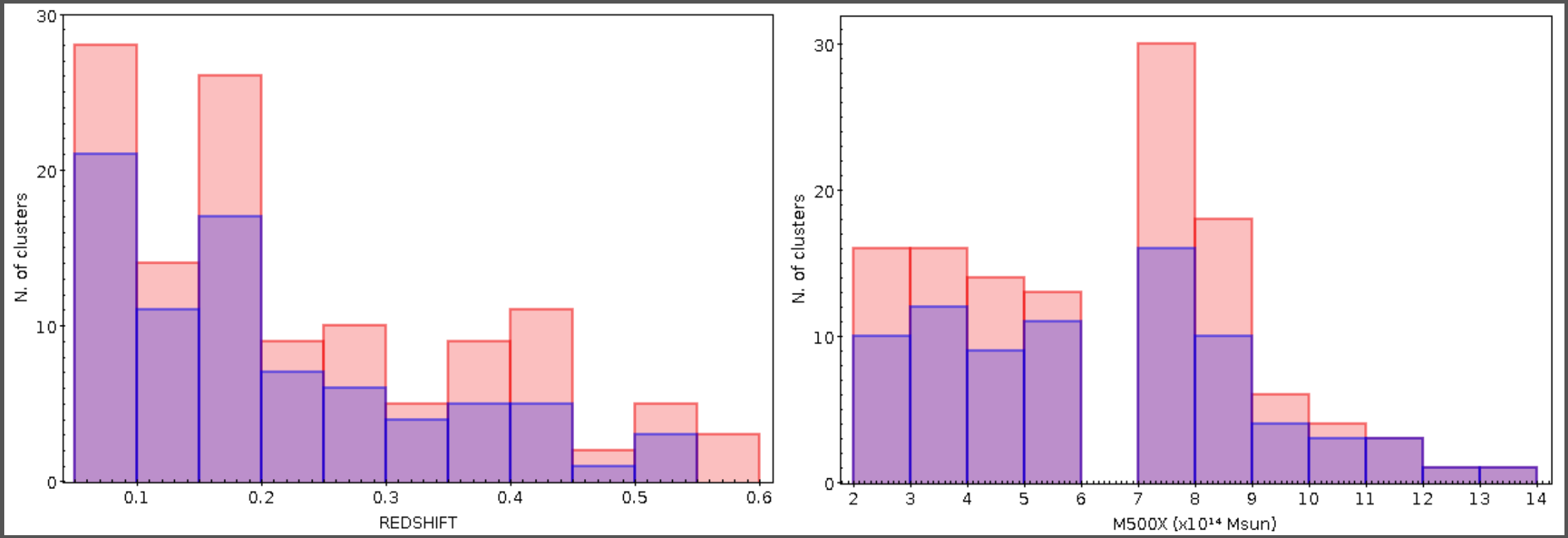


THE CHEX-MATE SAMPLE

THE CHEX-MATE SAMPLE

Cluster HEritage project with XMM-Newton – Mass Assembly and Thermodynamics at the Endpoint of structure formation (CHEX – MATE)

118 cluster SZ-selected (SNR > 6.5). Two subsamples: **Tier 1** (z <0.2), **Tier 2** (z > 0.2)



We consider a total of 75 clusters with at **least 50 confirmed members** within $R = r_{200c,ap}$ (Members selected with CLEAN, see Sereno+25)

MG-MAMPOSSt fit: mass estimates

For all clusters, we run a MCMC with 110000 points (10000 burn-in). **Flat uninformative priors (except for r_v)**

- four mass models: **NFW**, **Burkert**, **Hernquist**, **Einasto** $m = 3$
- two number density models: **pNFW**, **pHernquist**
- one general anisotropy model: **generalized Tiret**

Eight different combinations for each cluster in the sample

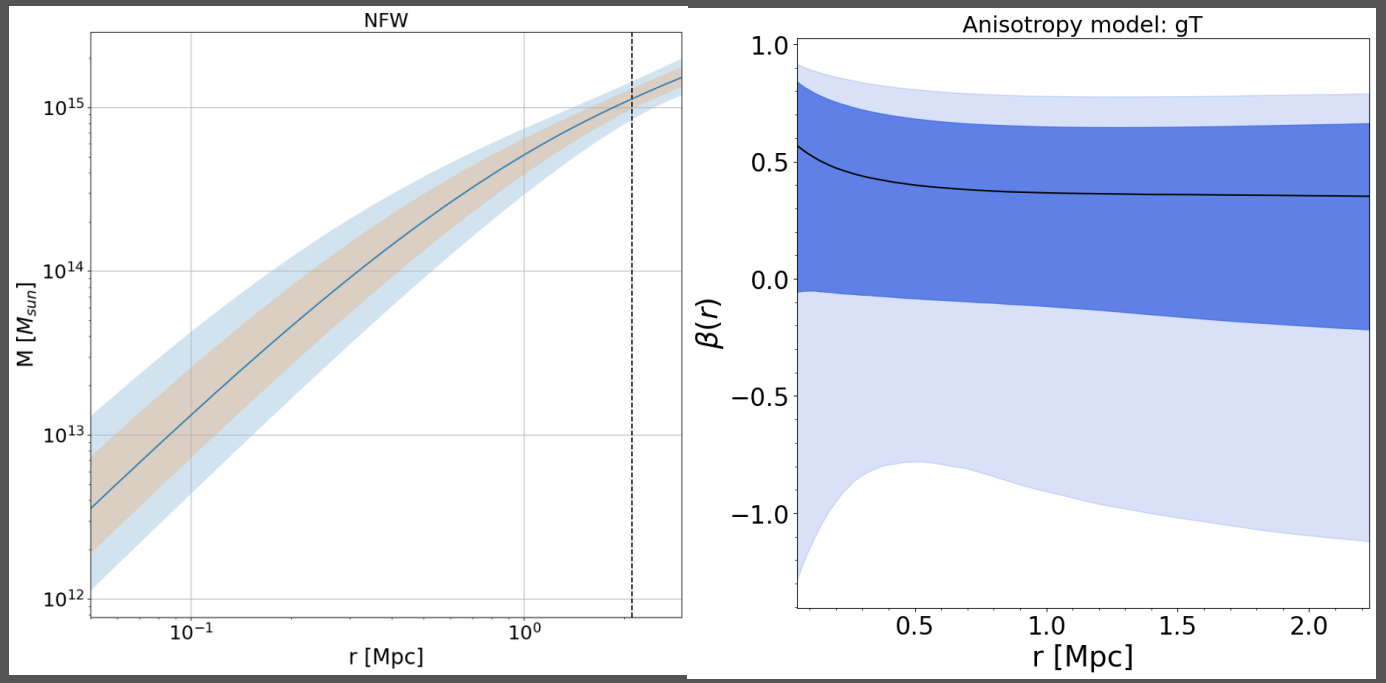
MG-MAMPOSSt fit: mass estimates

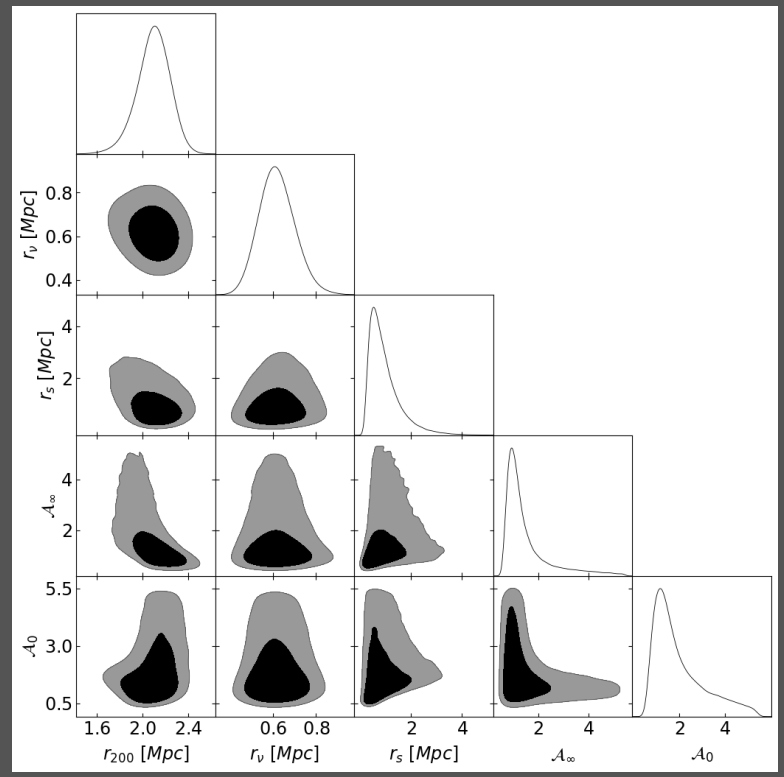
For all clusters, we run a MCMC with 110000 points (10000 burn-in). **Flat uninformative priors (except for r_ν)**

- four mass models: **NFW**, **Burkert**, **Hernquist**, **Einasto** $m = 3$
- two number density models: **pNFW**, **pHernquist**
- one general anisotropy model: **generalized Tiret**

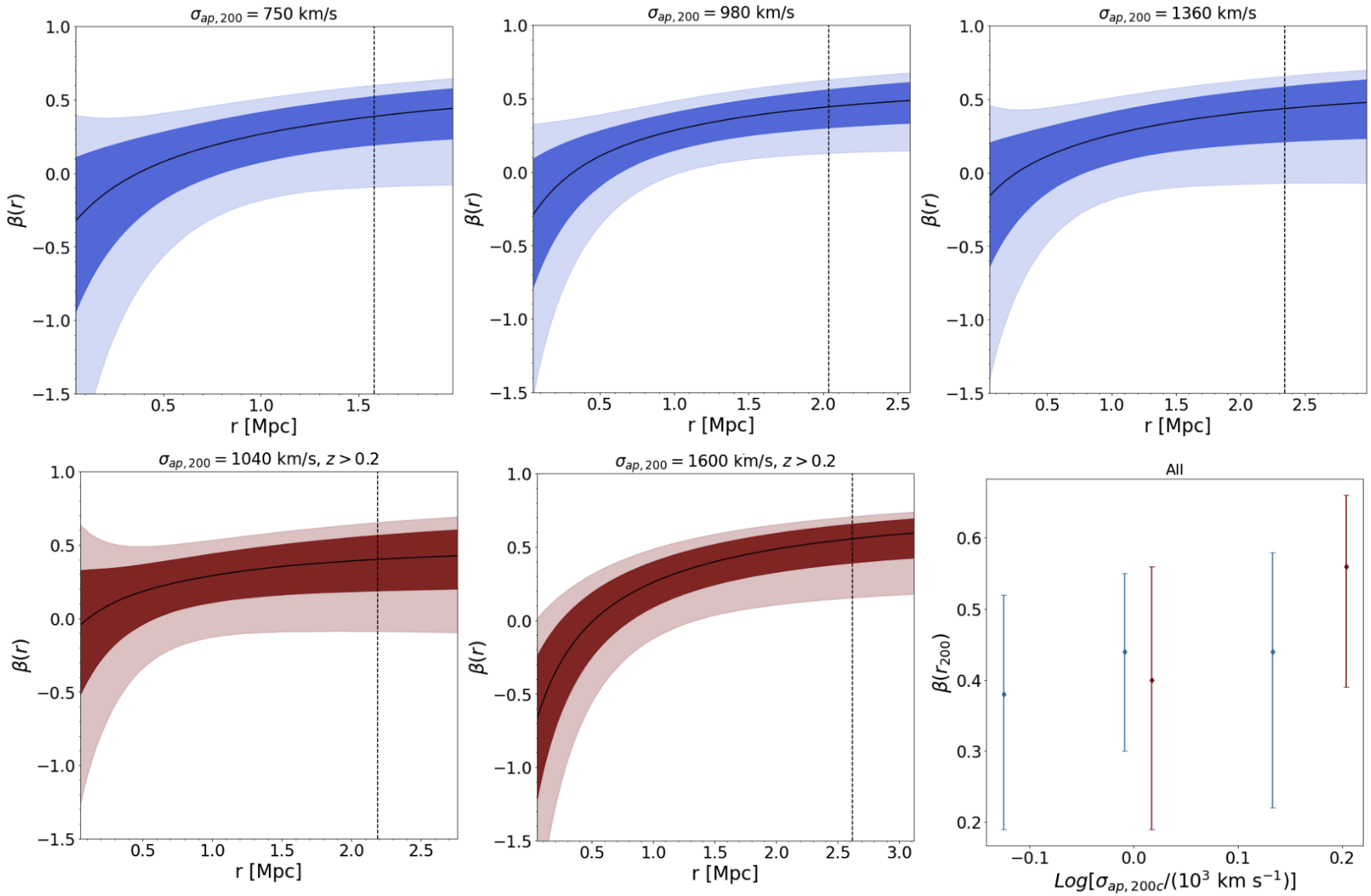
Eight different combinations for each cluster in the sample

Example: cluster PSZ2 G049.22+30.87





MG-MAMPOSSt fit: velocity anisotropy profiles



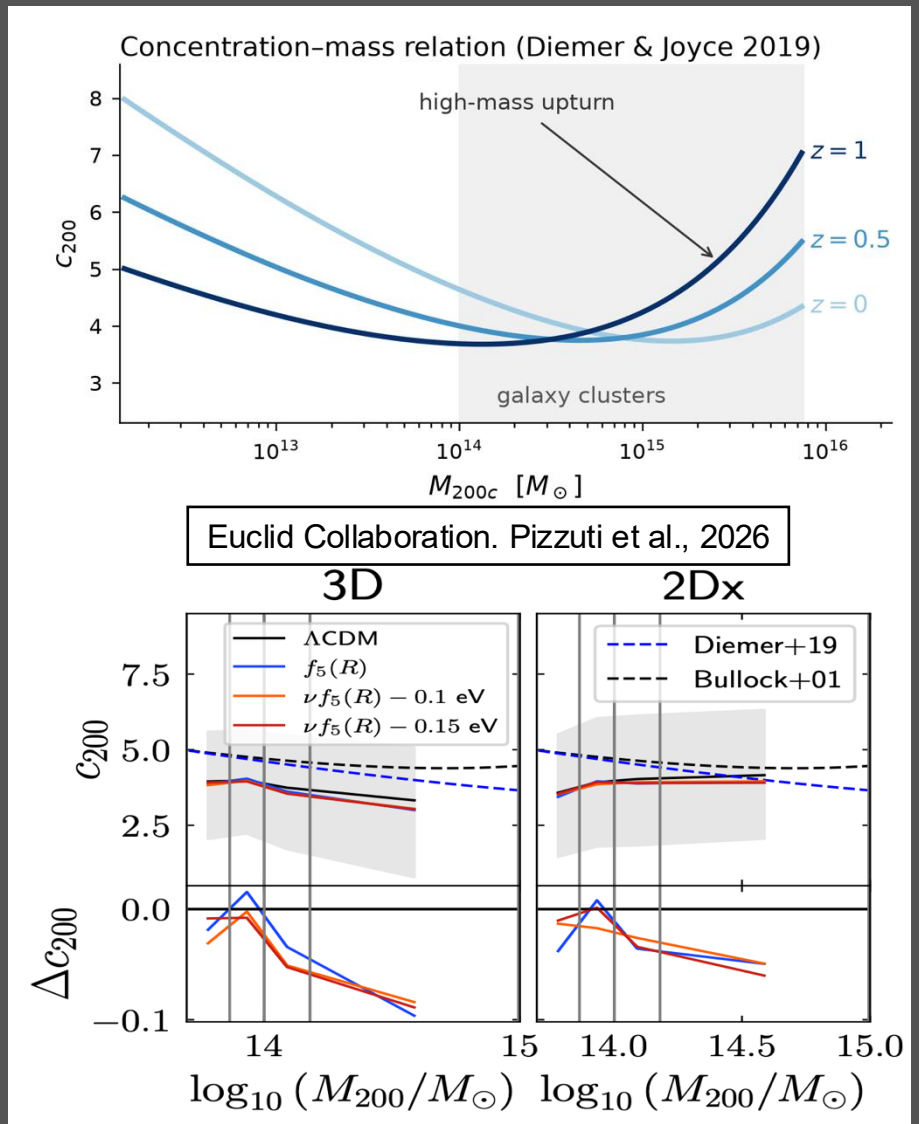
Stacking clusters in **bins of vdp and redshift**

- NFW assumed for the stacked clusters
- Slight tendence of more isotropic orbits for clusters with lower VDP

The concentration—Mass relation

Clusters are the end-point of the hierarchical structure formation process
Structural and scaling properties **connected to the cosmological model**

$c - M$ **relation:** scaling of the total mass (typically M_{200}) with the concentration $c_{200} = r_{200}/r_{-2}$

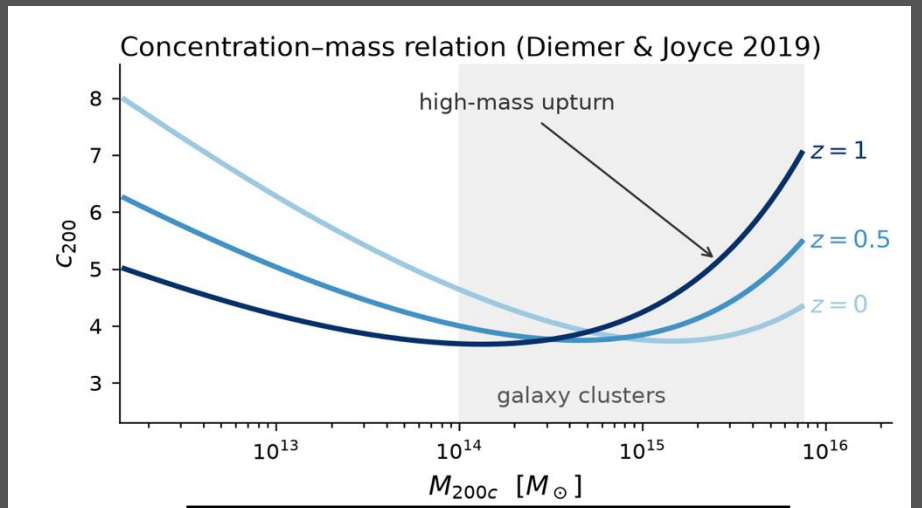


The concentration—Mass relation

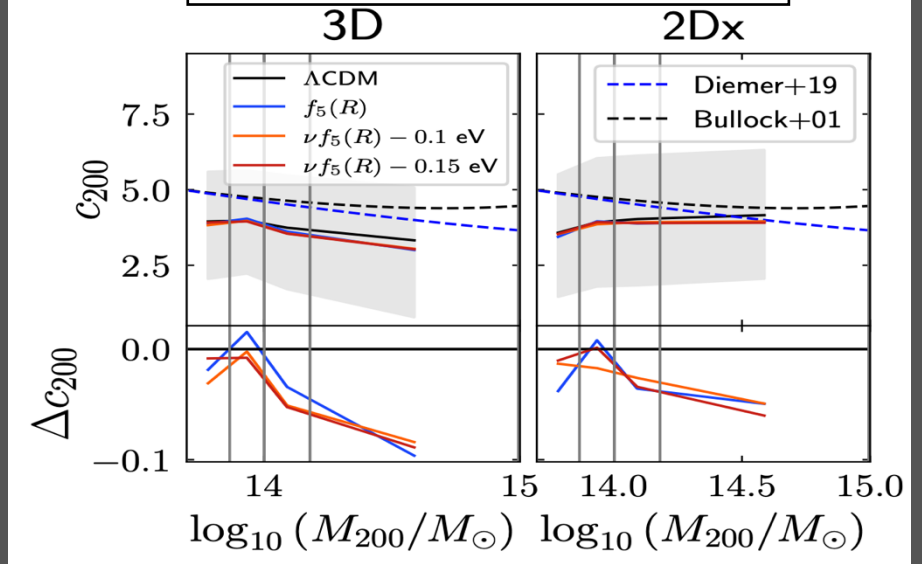
Clusters are the end-point of the hierarchical structure formation process
Structural and scaling properties **connected to the cosmological model**

$c - M$ relation: scaling of the total mass (typically M_{200}) with the concentration $c_{200} = r_{200}/r_{-2}$

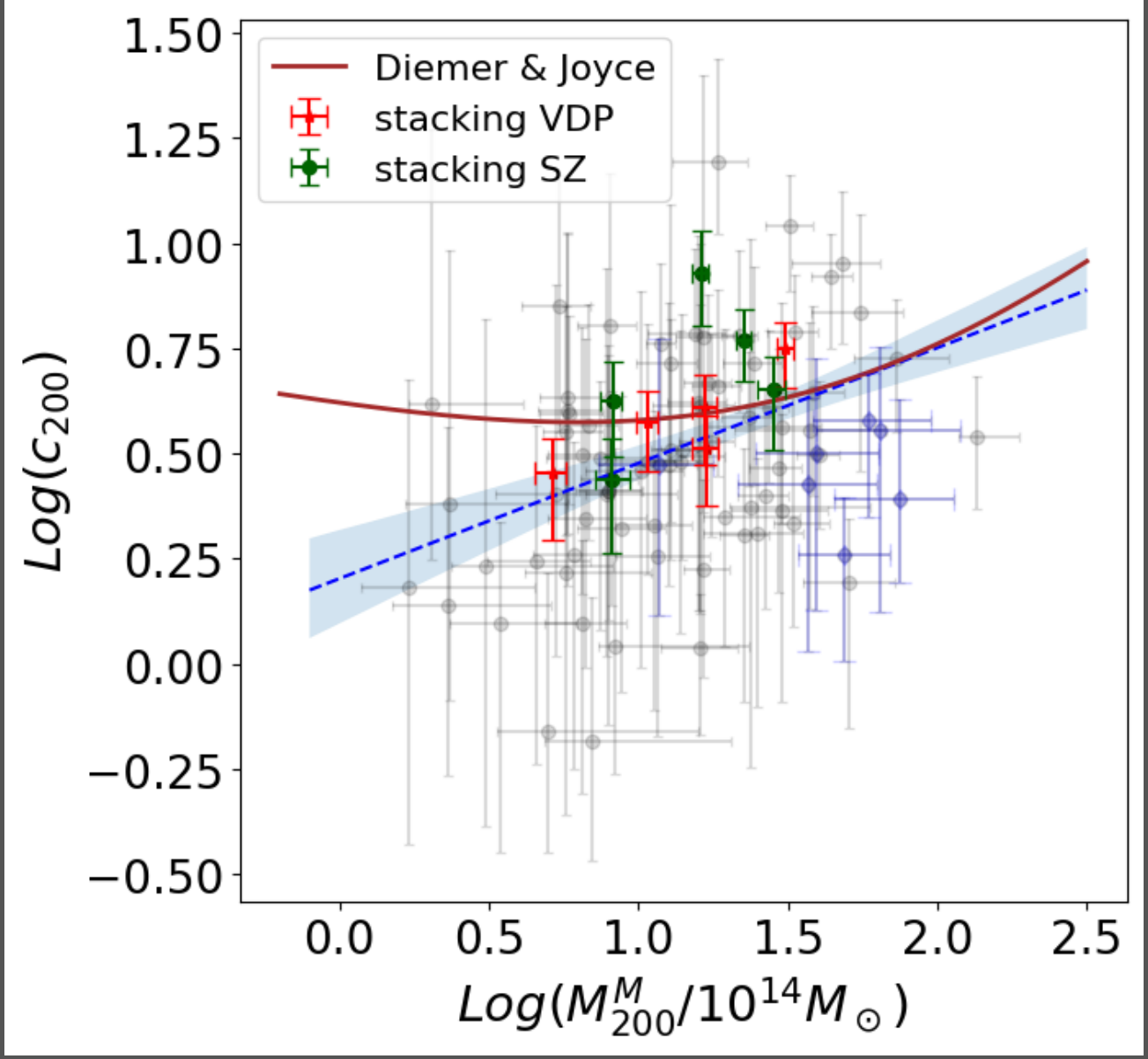
- Early-forming haloes **more** concentrated → weak negative mass dependence, mild redshift evolution
- **Cluster regime**: $c_{200} \sim 3 - 5$ for $\sim 10^{15}\, M_{\odot}$, depending on z
- **Scatter at fixed mass** ≈ 0.1–0.15 dex, driven by the spread in formation time and by departures from equilibrium.
- **Upturn at the highest masses**: most massive clusters are assembling ***now:*** larger c_{200}, disequilibrium (Diemer & Joyce 2019, Ishiyama+2021).



Euclid Collaboration. Pizzuti et al., 2026

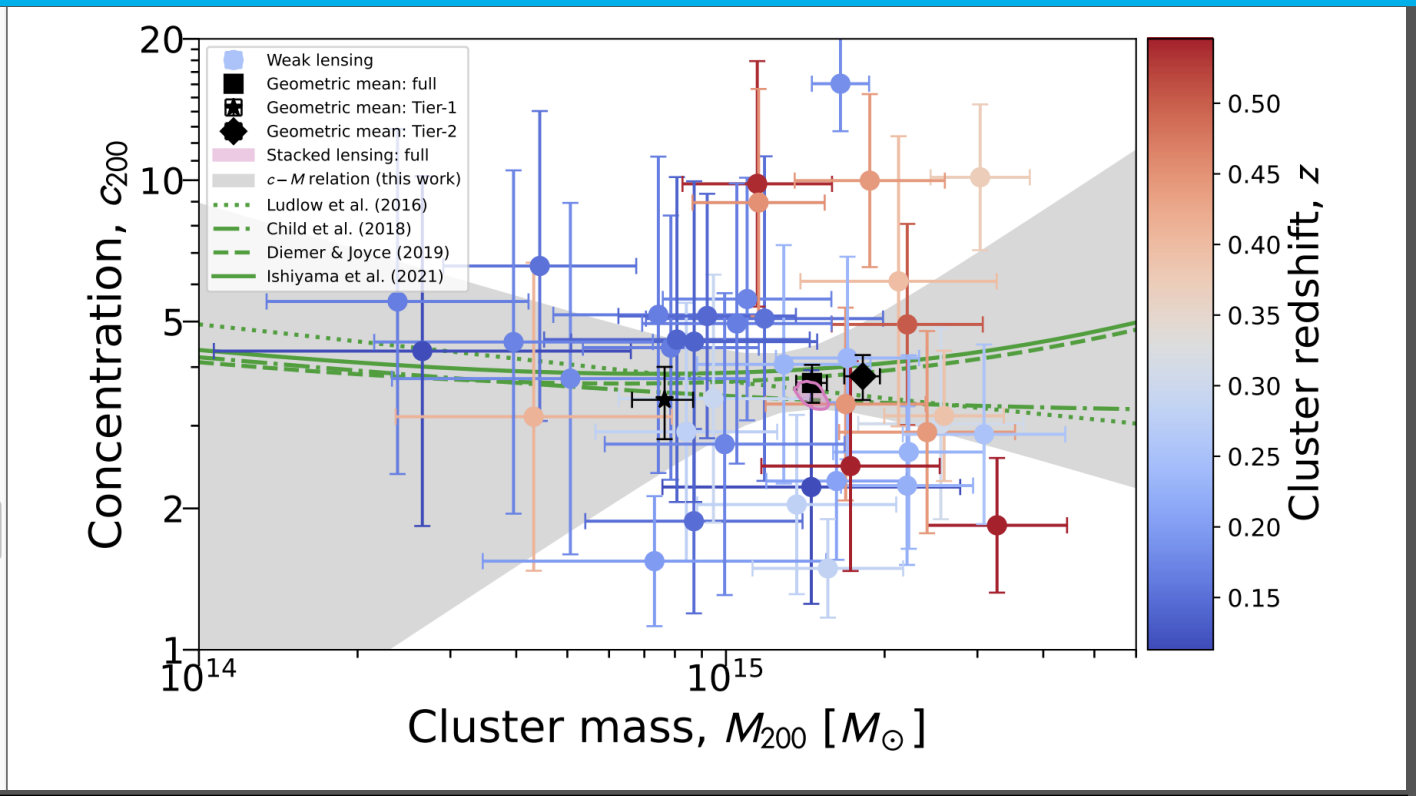


The c-M relation of the kinematic sample (Pizzuti+2025)



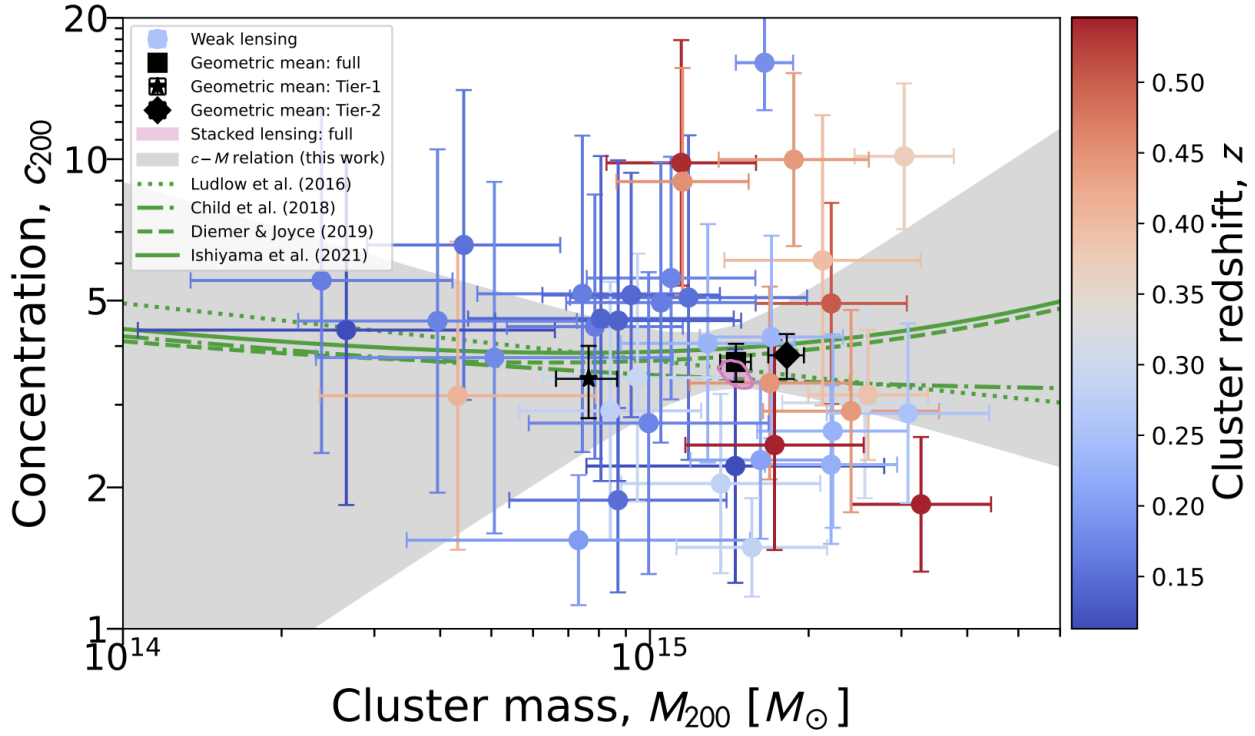
- Slightly rising trend found by a ODR linear fit
- In agreement with theoretical prediction of Diemer&Joyce, 2019
- Red points from stacking analysis

What do we have now?



Weak lensing data for 41 CHEX-MATE clusters from the AMALGAM program (Umetsu et al., 2026)

What do we have now?

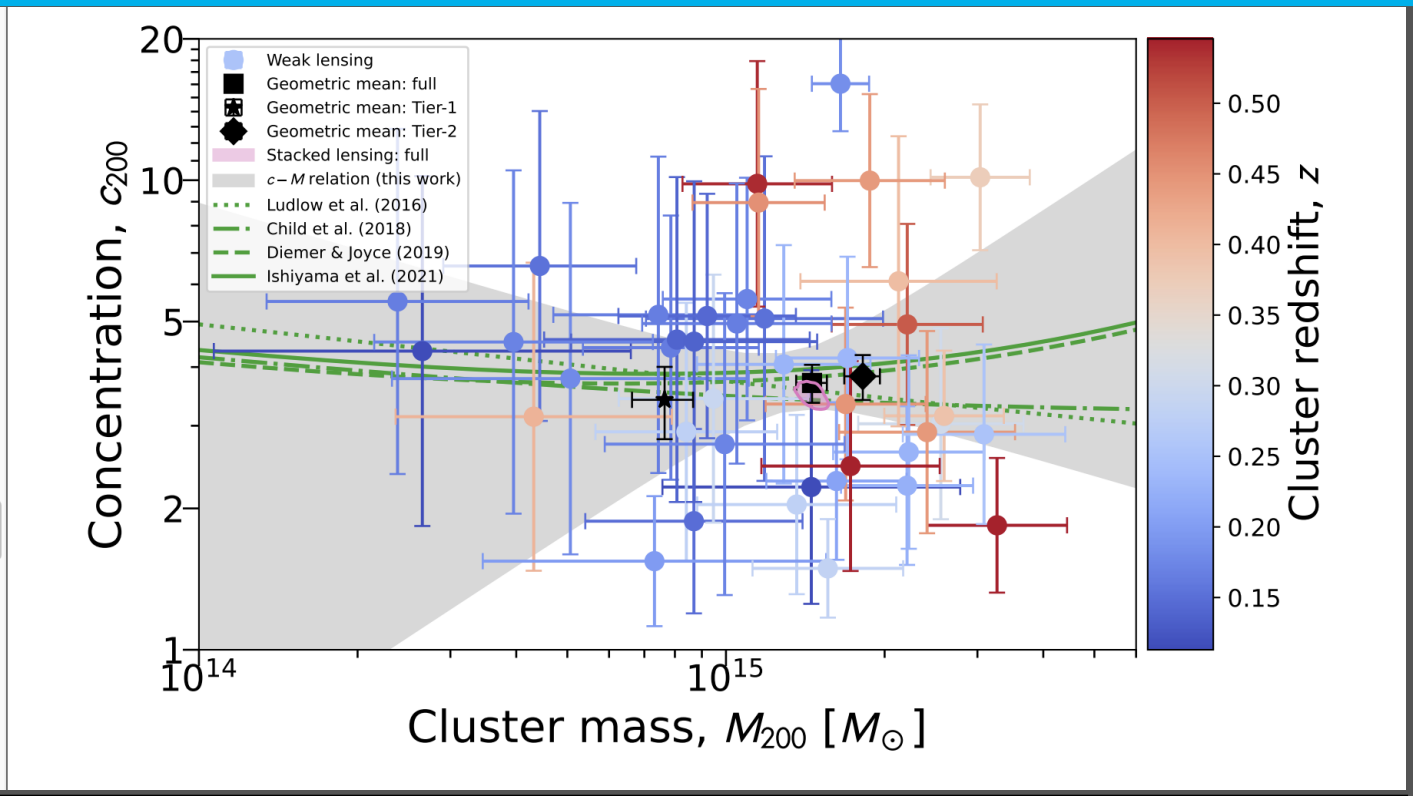


Weak lensing data for 41 CHEX-MATE clusters from the AMALGAM program (Umetsu et al., 2026)

+

An updated catalog of member galaxies' spectra for the CHEX-MATE sample by Mauro

What do we have now?



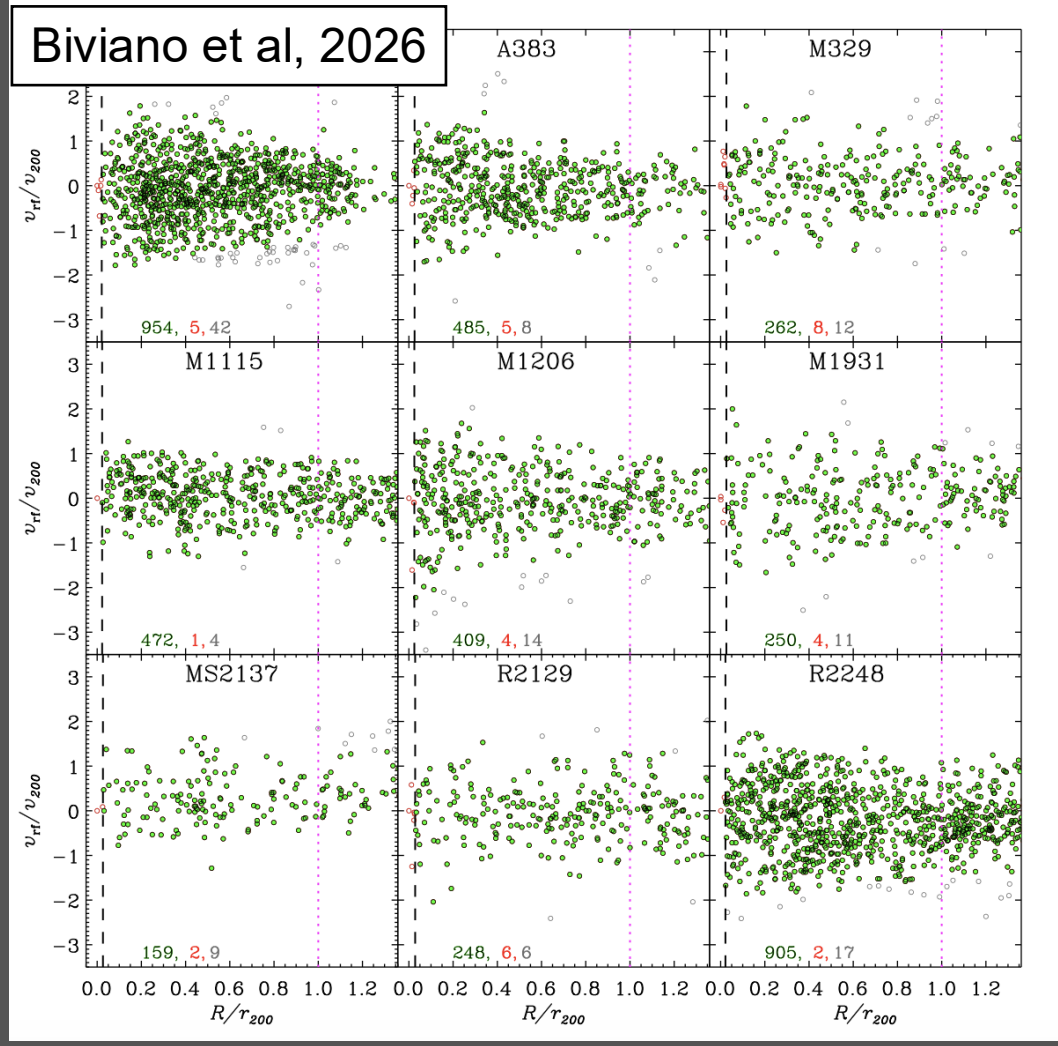
Weak lensing data for 41 CHEX-MATE clusters from the AMALGAM program (Umetsu et al., 2026)

+

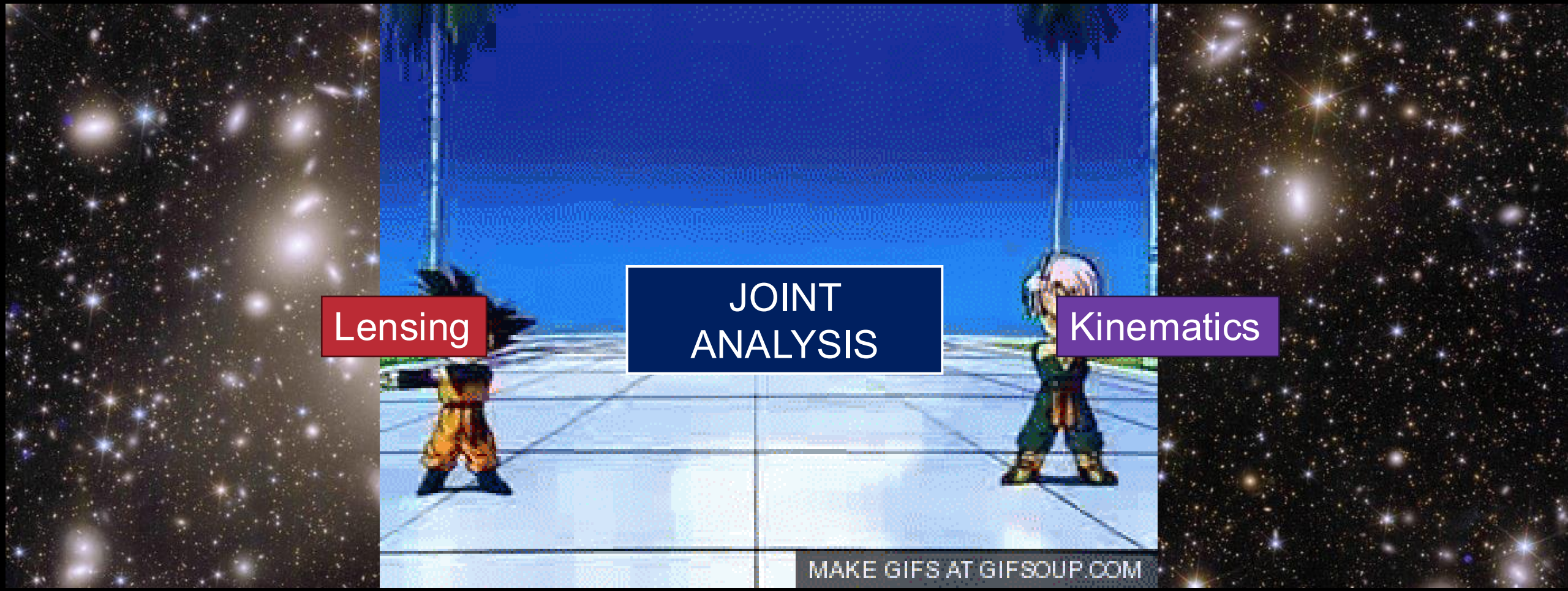
An updated catalog of member galaxies' spectra for the CHEX-MATE sample by Mauro

+

Biviano et al, 2026

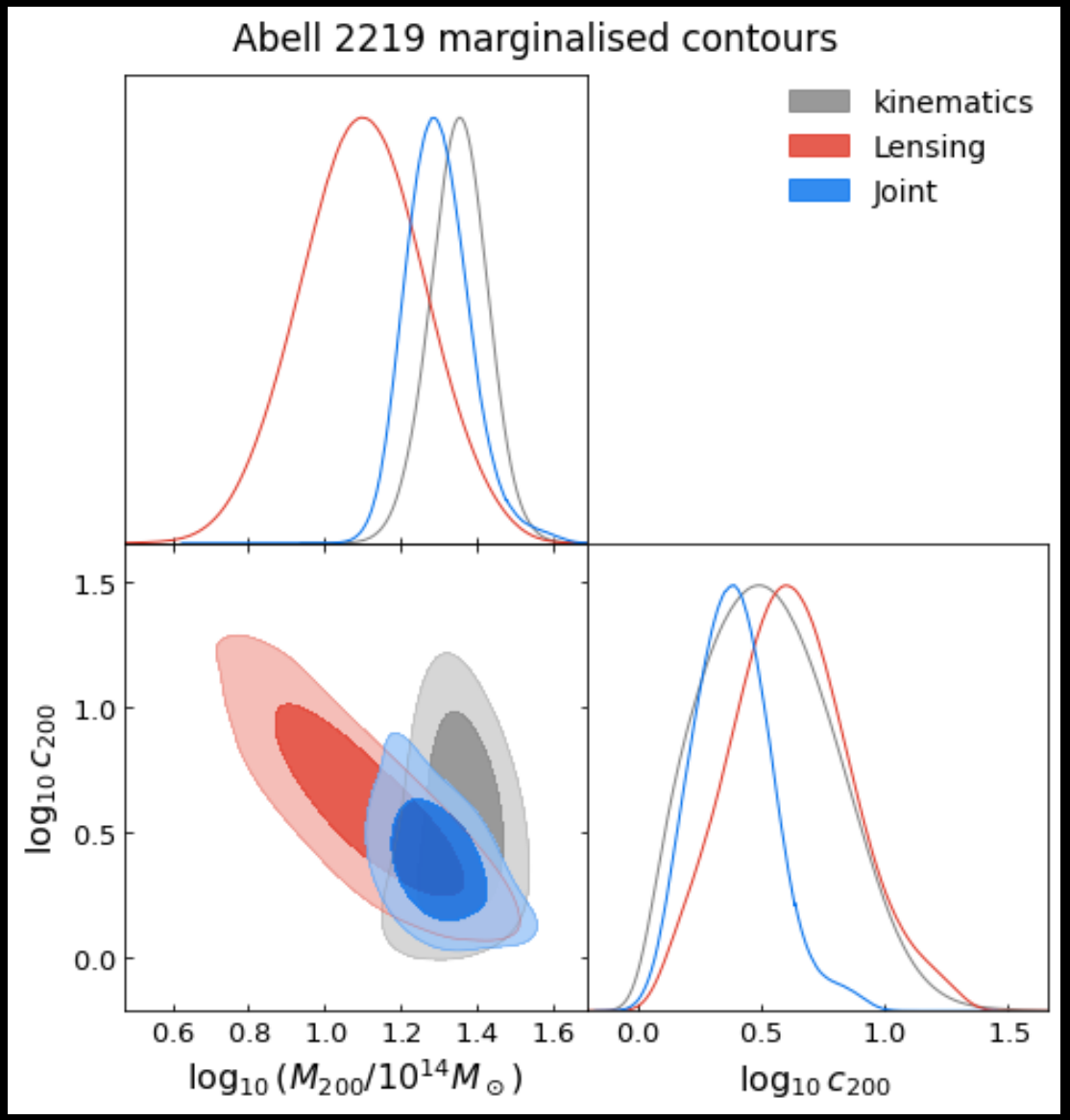


NINE CLASH-VLT clusters with high-quality kinematics, weak+strong lensing data



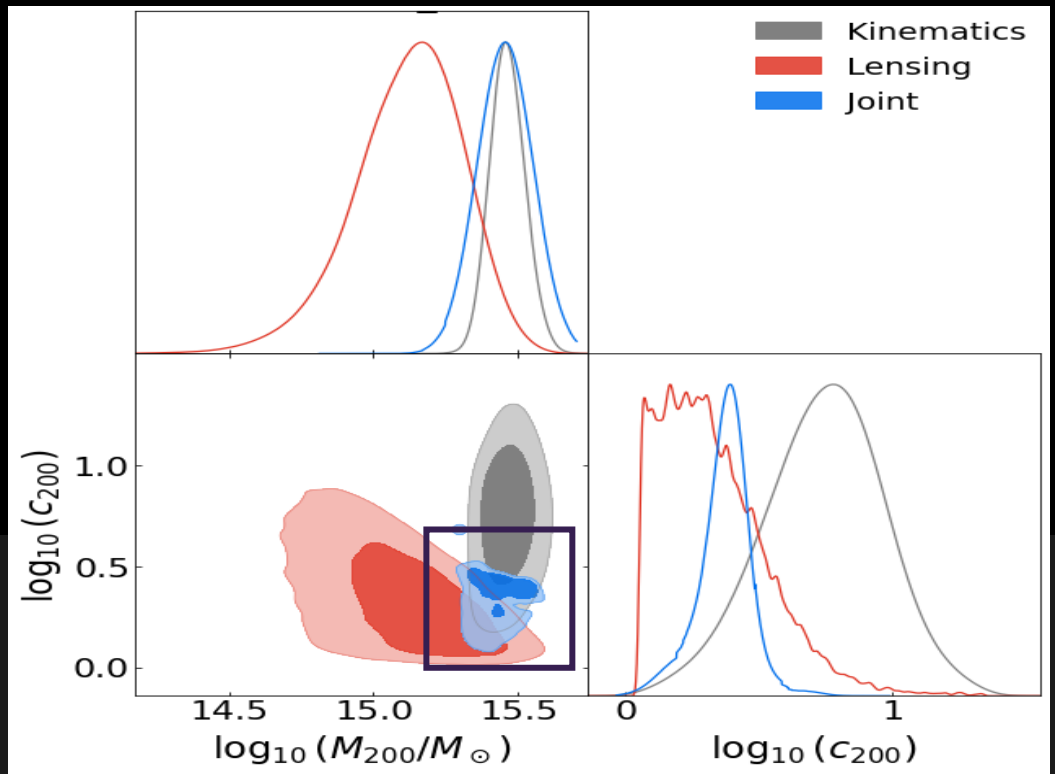
Let’s put things together!

Combine lensing and kinematics mass profile estimates to obtain a more precise scaling relation



Joint analysis: weigh the lensing posterior with the kinematical likelihood (importance sampling)

$$P(\theta|\ \text{lensing} + \text{kinematics}) \propto P(\theta|\ \text{lensing}) \times \mathcal{L}(R, v_z\} \mid \theta)$$

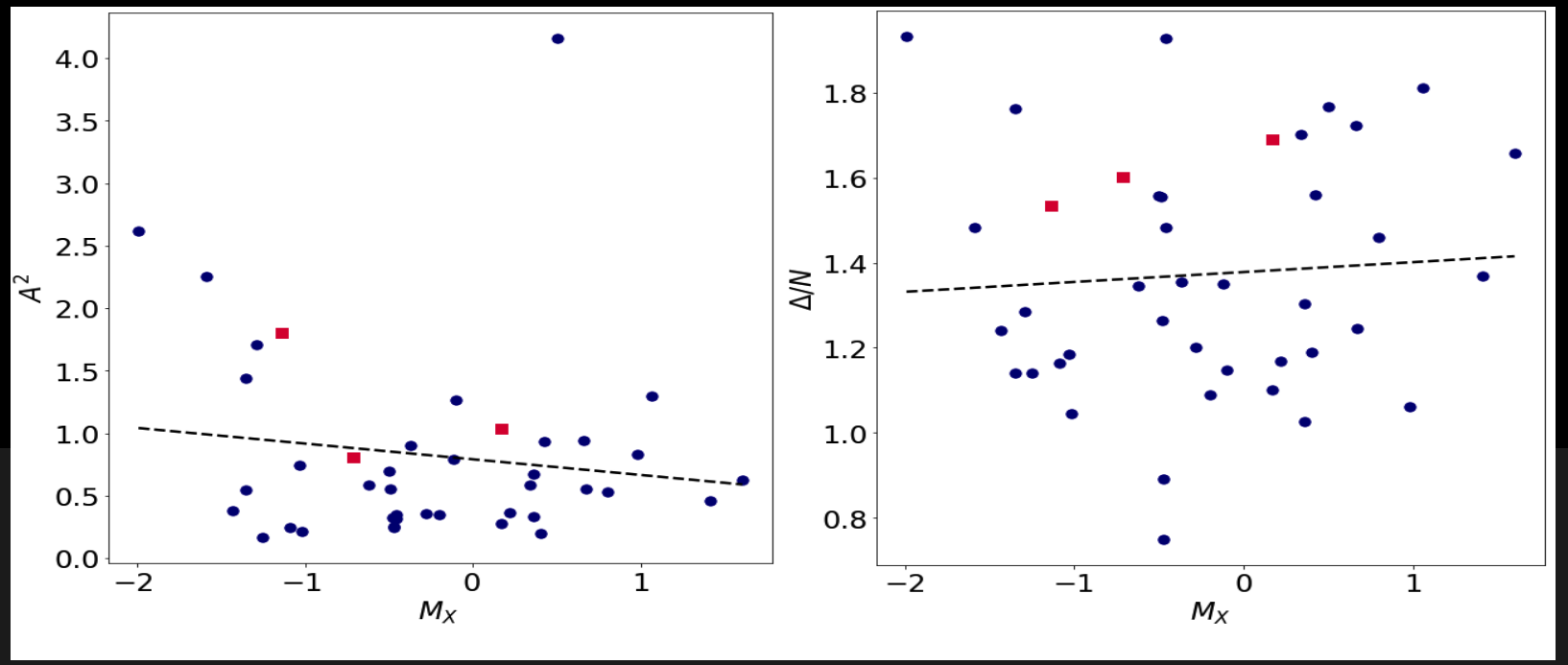


The combination should be done cautiously! Not all posteriors agree.

Systematic analysis of the lensing and kinematics results as a function of **dynamical-state indicators**



- **X-ray morphological parameter M_X** (Campitiello+2022)
- **The Anderson-Darling coefficient A^2** (non-Gaussianity of VDP)
- **The Dressler-Shectman (DS) test statistics Δ/N** (substructures)



Almost no correlation among the kinematics and X-ray indicators

Probing different aspects of the dynamical state

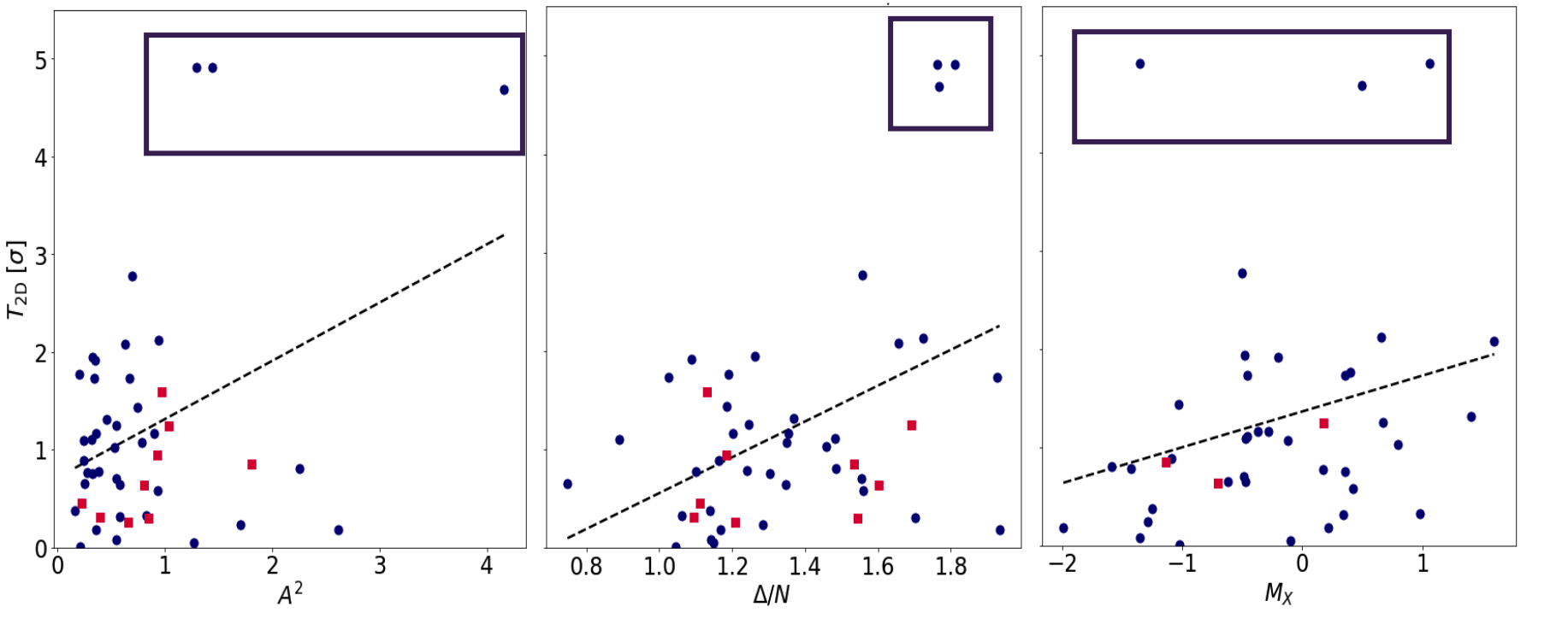
Systematic analysis of the lensing and kinematics results as a function of **dynamical-state indicators**



- **Tension between lensing and kinematics:**

$$T_{2D} = \left[\Delta\mu^{T}\left(C_{lens} + C_{dyn}\right)^{-1}\ \Delta\mu\right]^{\frac{1}{2}}$$

Weak correlation with the dynamical-state indicator



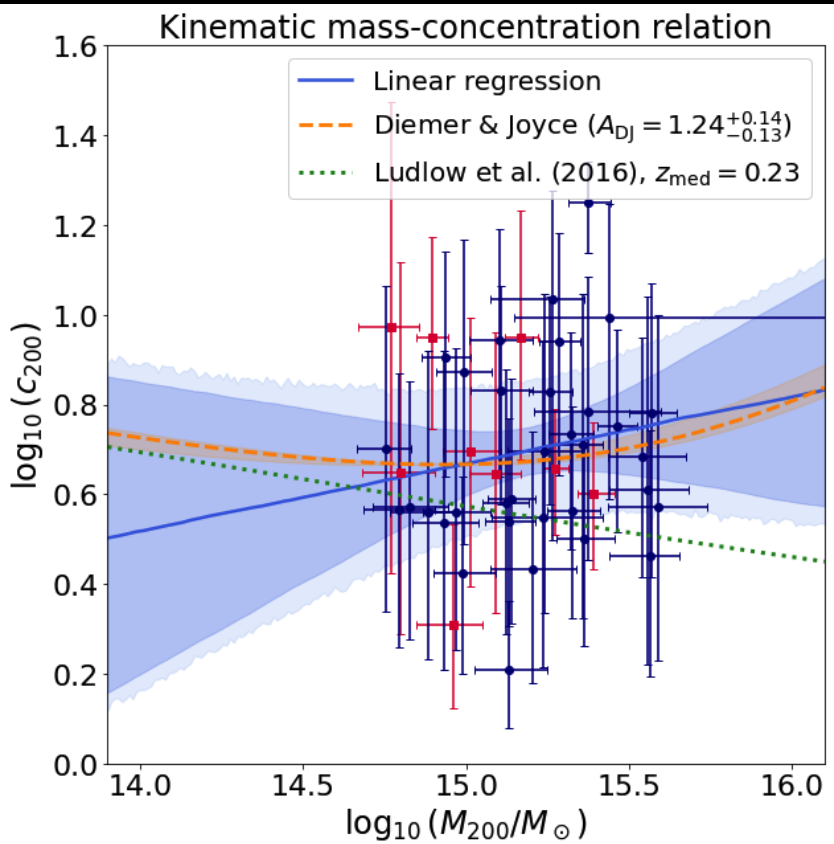
For three clusters **no joint posteriors!**

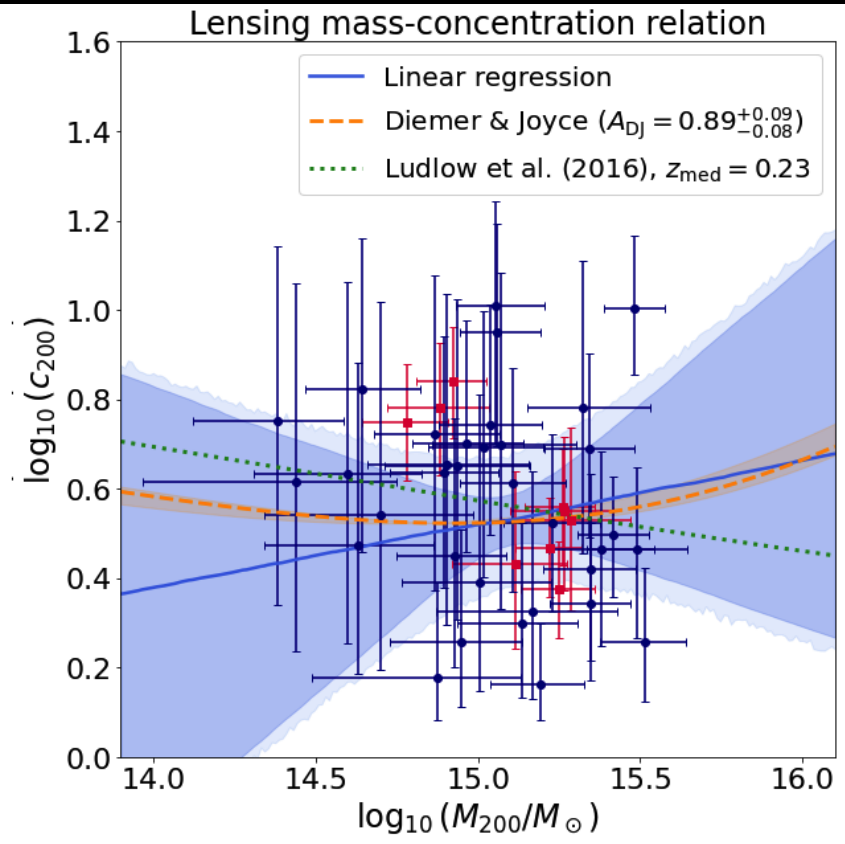
Kinematically disturbed

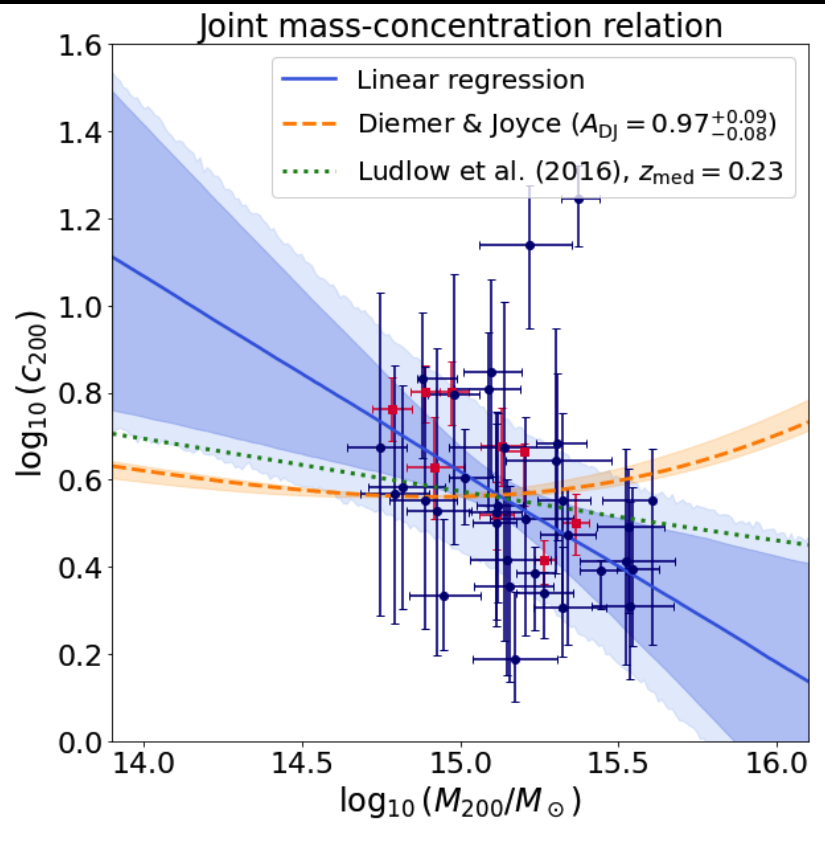
$$A^2 > 1, \qquad \frac{\Delta}{N} > 1.6$$

One appear to be **regular in X-ray** morphology (A1689)

The c—M relation: all clusters considered 35 CHEX-MATE + 9 CLASH



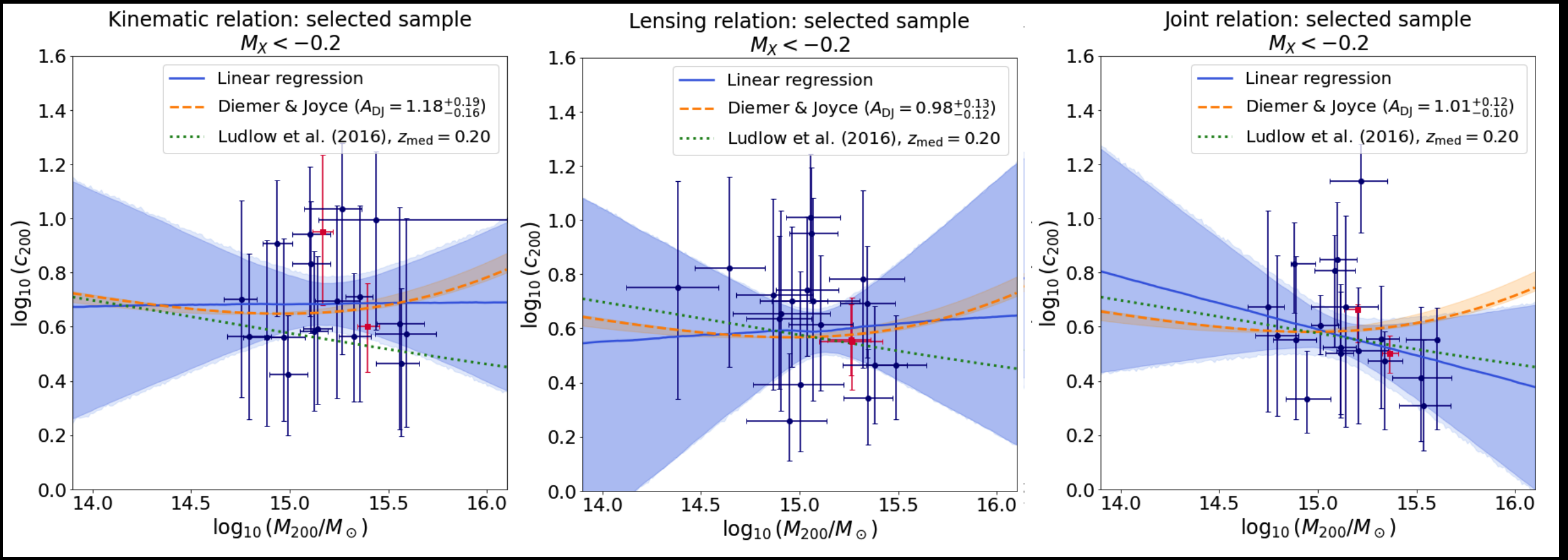




Hierchical Bayesian fit accounting for selection biases and intrinsic scatter.
The joint relation reduces the scatter w.r.t. to the single-probe relation – **decreasing trend**
Consistent with the D&J prediction (normalisation $A_{DJ} = 1$)

The kinematic c—M relation exhibits the hint of increasing trend in the median, but consistent with a flat behavior when uncertainties are inculded

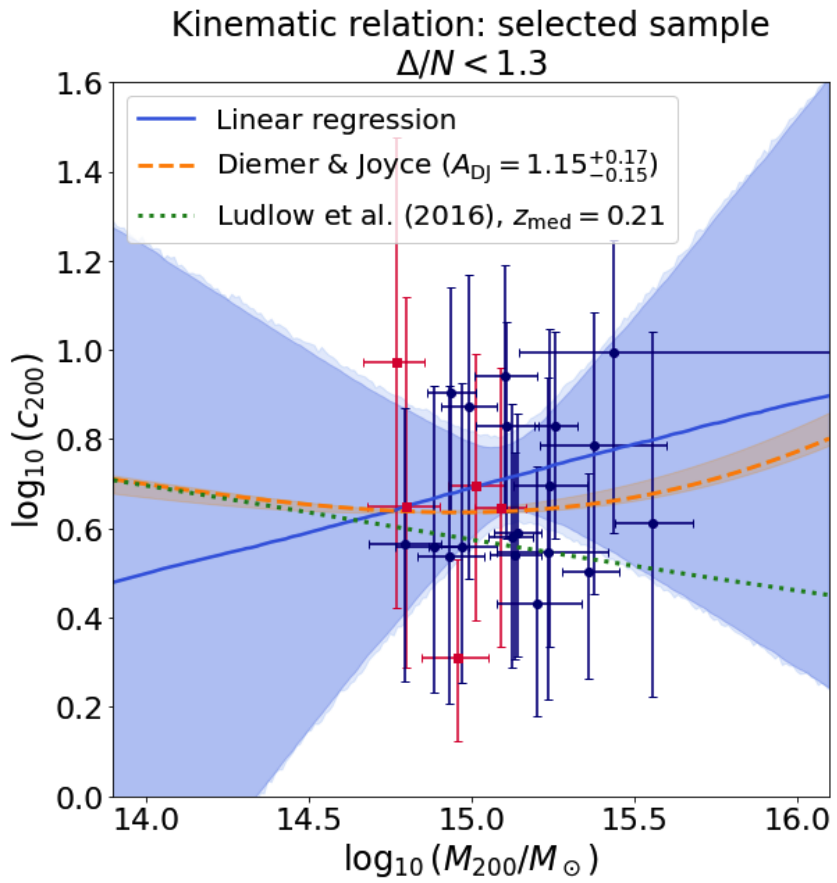
The c—M relation: X-ray selection (when possible)

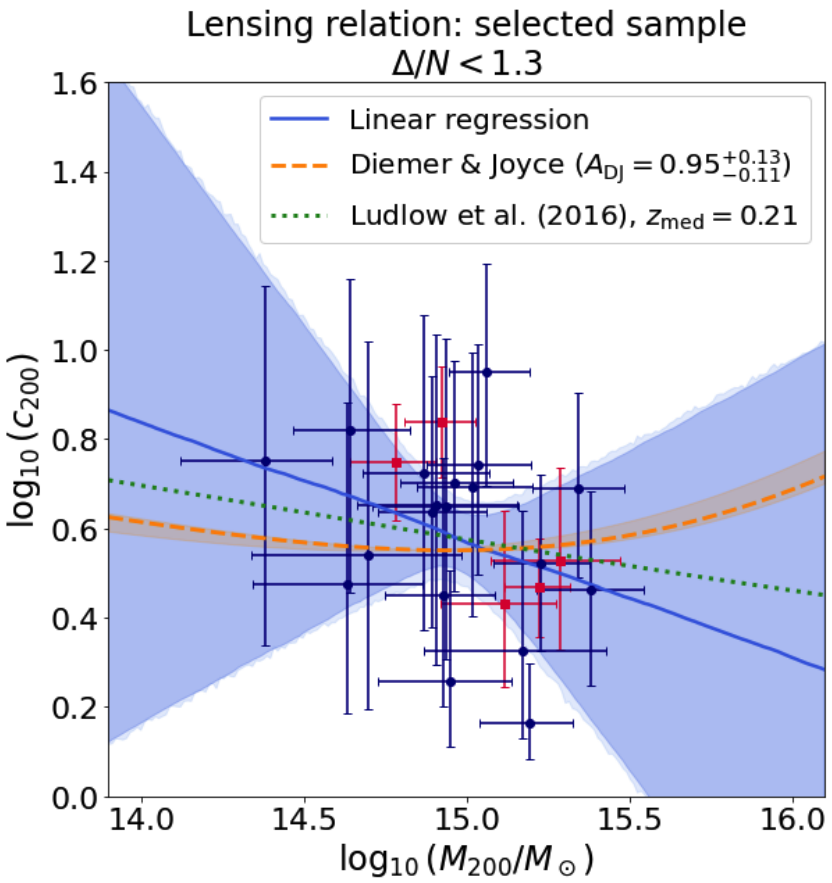


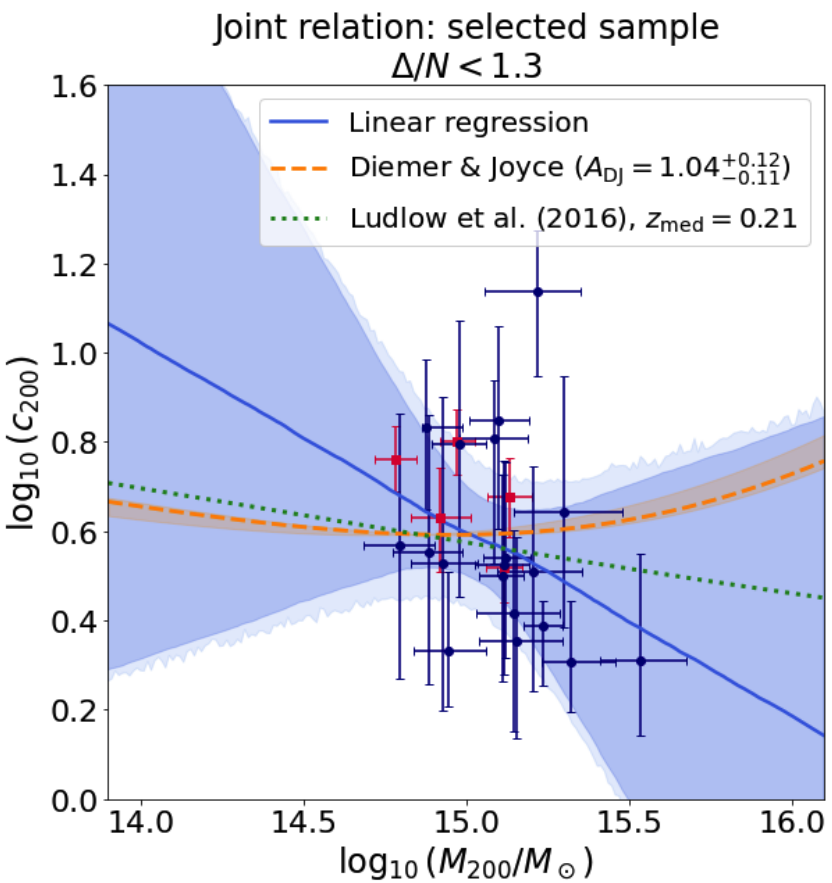
The kinematic c—M relation is consistent with a flattening

No significant changes in the joint relation

The c—M relation: DS selection



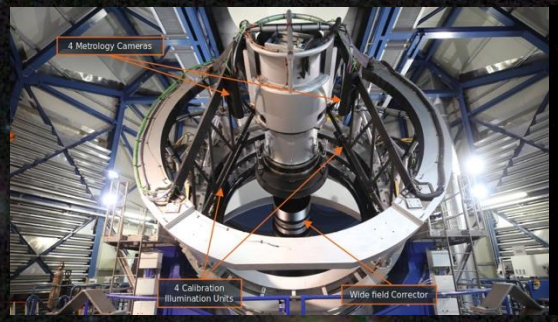


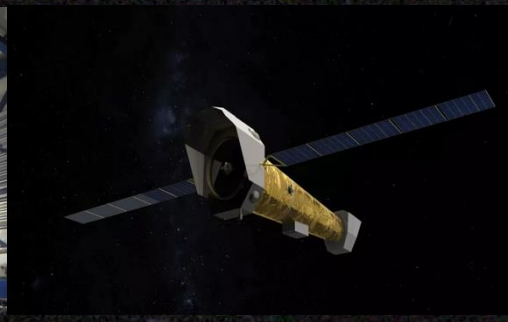


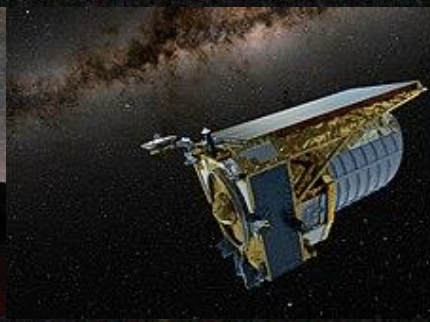
Decreasing trend in the joint fit enhanced

No overall preference of the linear model with respect to the D&J relation

Conclusions: a bright future for multiwavelength cluster studies?





The increase of quality and quantity of data allows for detailed studies of cluster properties

Next steps: add X-ray / radio information. **We need to be very careful!** Measurement correlations and selection effects

Combination to get tight constraints on **gravity**, the **dark sector** and **cosmic assembly**, but also **galaxy evolution in dense environments**.

Extending to many clusters requires **accurate calibration of systematics**!

The KRONOS project

KRONOS

Kinematic mass Reconstruction and Orbital Non-equilibrium Observatory for Structures

Package built to collect several routines for kinematical analysis. It includes:

- **Membership selection** and **projected phase-space generation (CLEAN, +Singed?)**
- **Number density fitting**
- **Mass/mass profile estimates**: aperture velocity dispersion, MG-MAMPOSSt (+ML?)
- **Diagnostics** of systematics uncertainties/ relaxation state
- **Scaling relation**: hierarchical Bayesian linear regression based on the LIRA model of Sereno, 2016)

The KRONOS project

KRONOS

Kinematic mass Reconstruction and Orbital Non-equilibrium Observatory for Structures

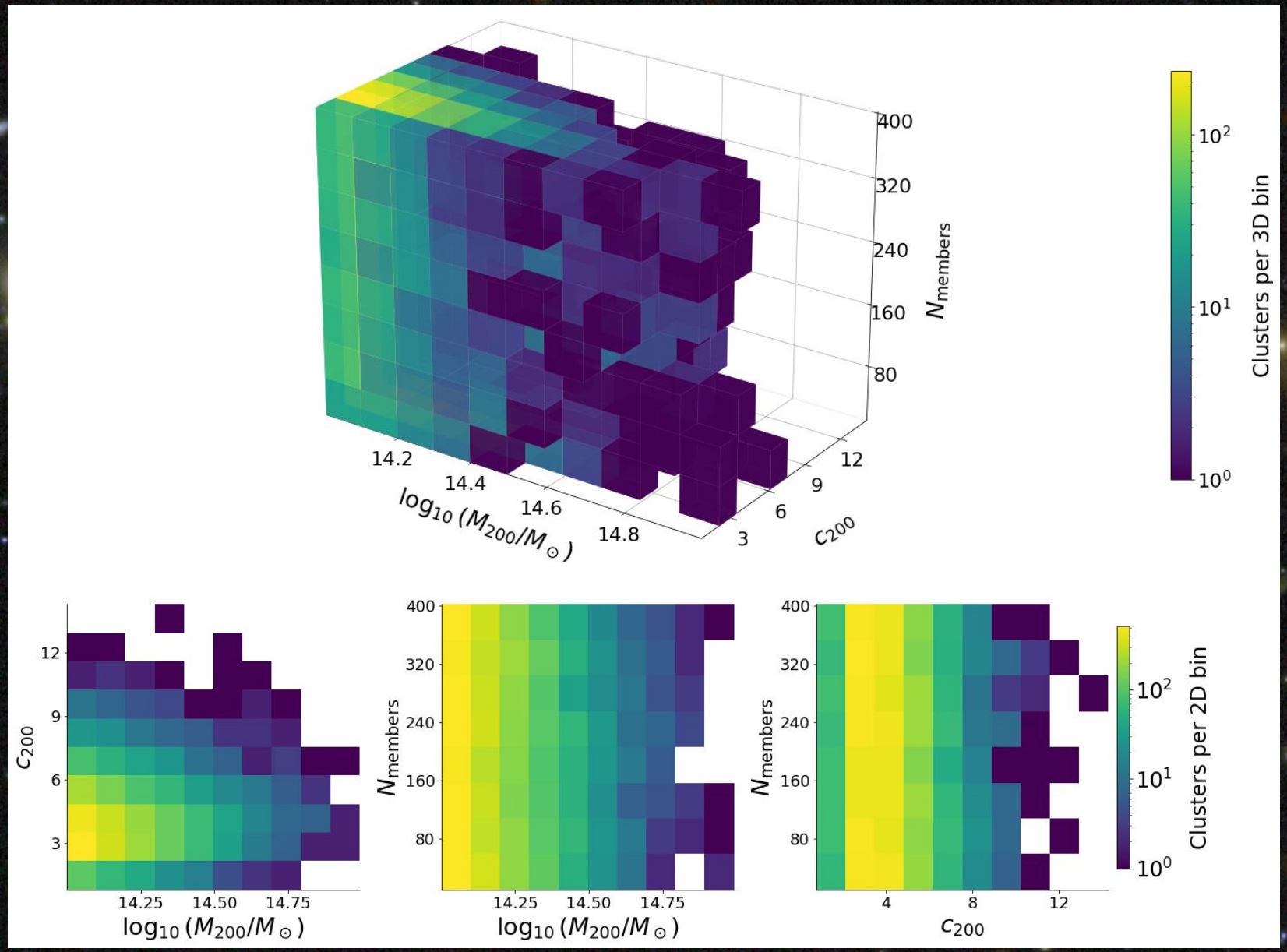
Full calibration of a distribution of biases in mass and concentrations given a set of disturbance proxies

$P(b_M, b_c \mid N_{members}, \vec{d}_{kin})$

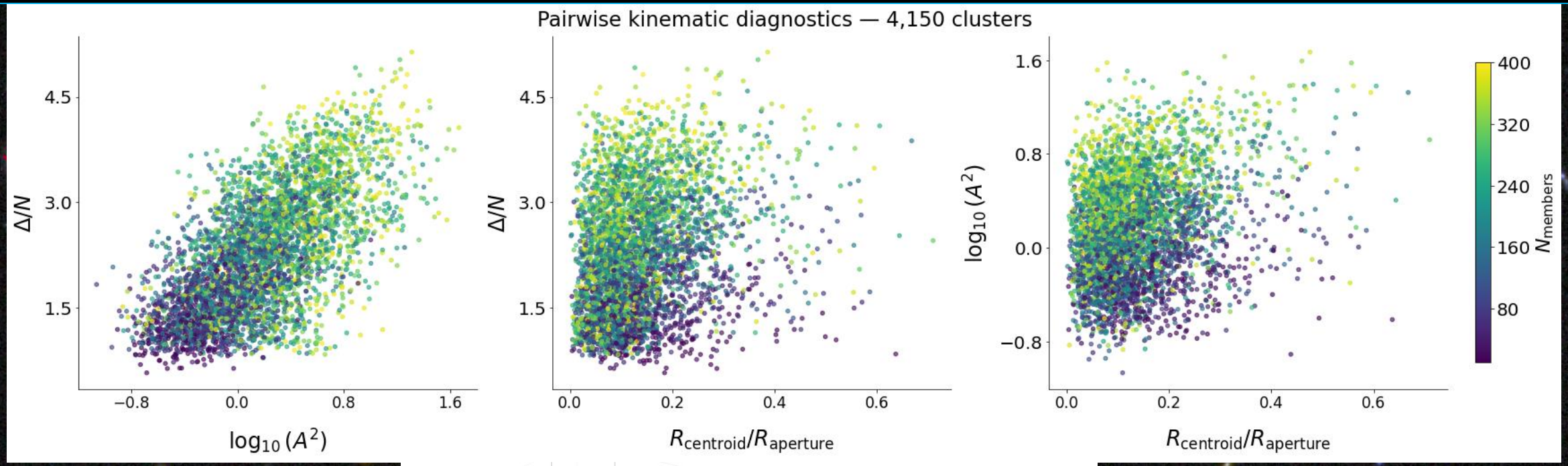
Generated 10^4 isolated mock clusters at a reference $z = 1$ varying:

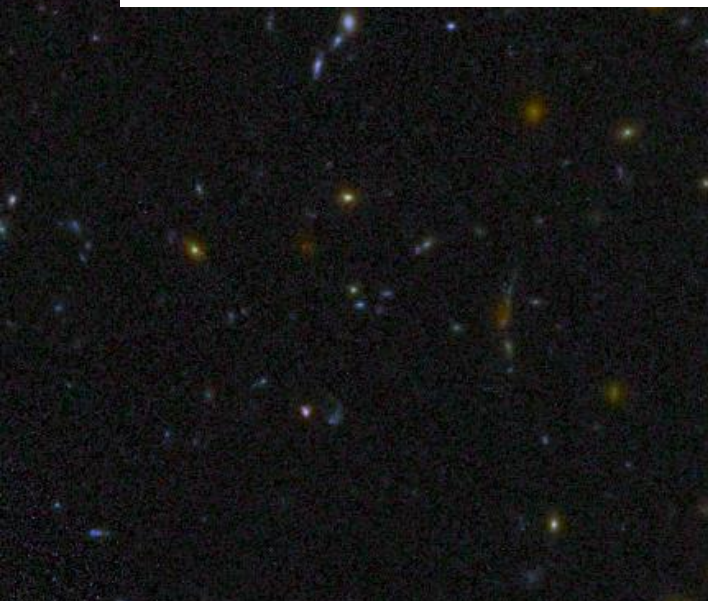
- ✓ M_{200c}, c_{200c} from a Tinker mass function and a Diemer&Joyce *c*—*M* relation (assuming 0.15 scatter in dex)
- ✓ the **number of members** $N \in [10, 400]$
- ✓ the **weight of a secondary component** of the velocity distribution $\in [0\%, 40\%]$, and its offset $\delta v / v_{200} \in [-2, 2]$
- ✓ the **number, size and cluster-centric distance** of substrucutres
- ✓ the **shift of the observational center** w.r.t. to the true cluster center $\delta r / r_{200} \in [0, 0.2]$

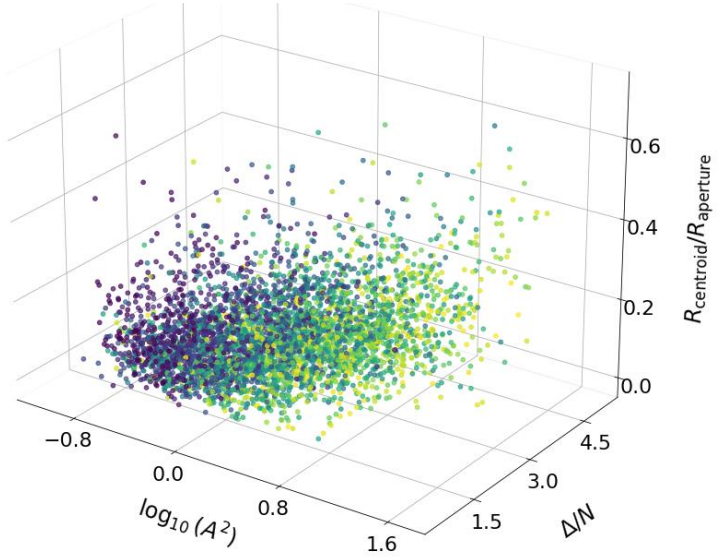
The KRONOS project

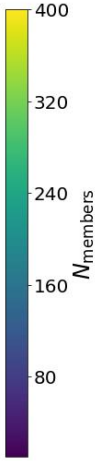


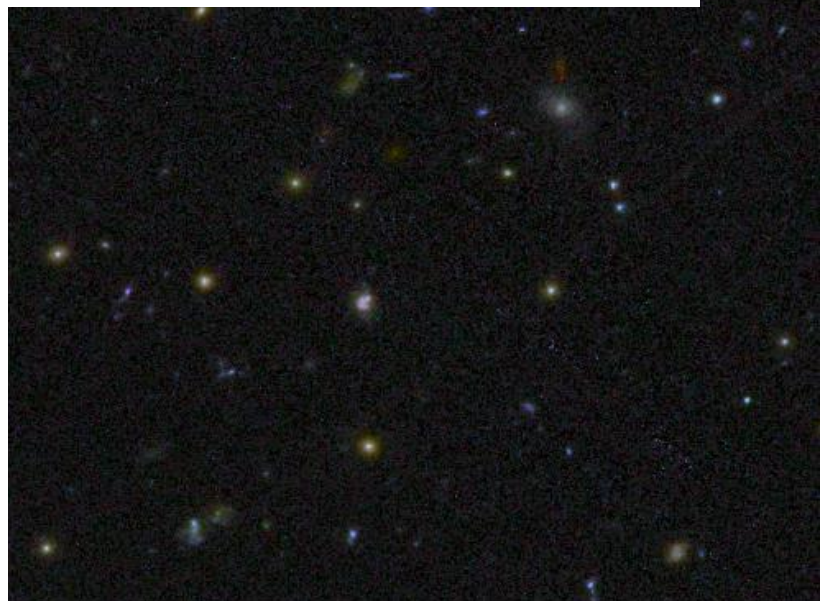
The KRONOS project





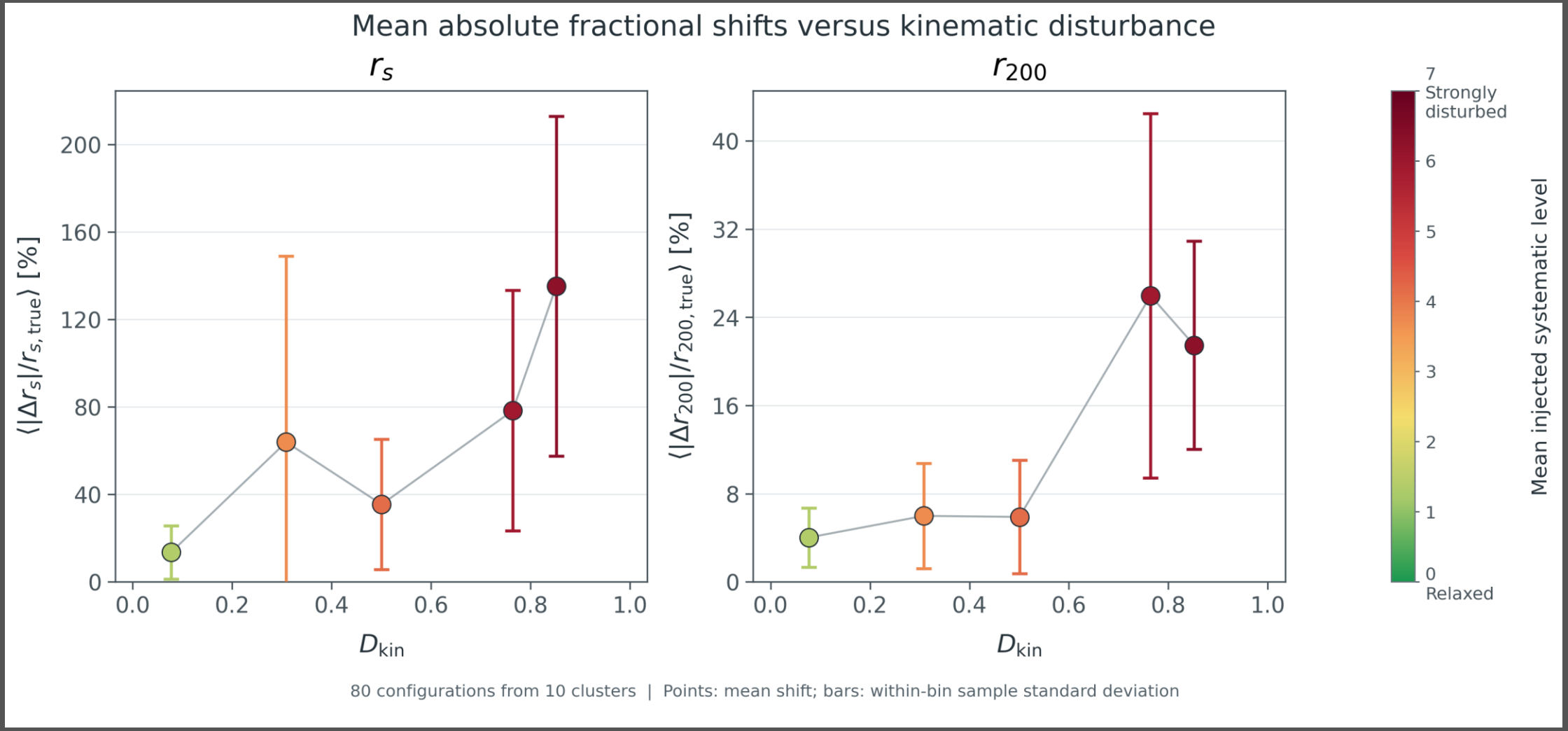






Testing a provisional combined score of kinematical disturbance

Evident correlation between the score and the bias in the mass reconstruction. Heuristic calibration!



Conclusions: a bright future for multiwavelength cluster studies?

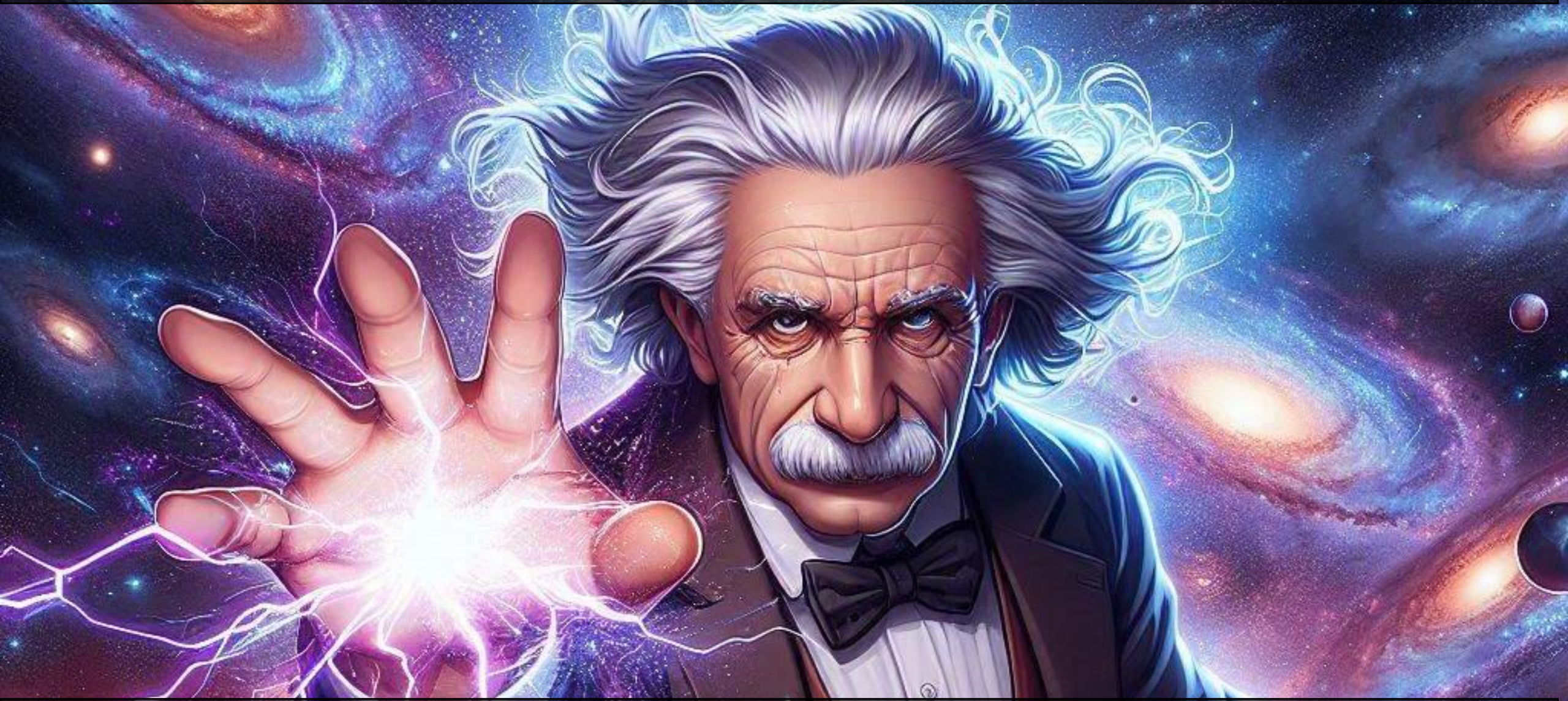
Full calibration of a distribution of biases in mass and concentrations given a set of disturbance proxies
$P(b_M, b_c \mid N_{members}, \vec{d}_{kin})$

The next steps:

- Determine the bias distribution with a Neural Network?
- Test with full-physics cosmological simulations (e.g., TNG, The Three Hunderd)
- How does the distribution change for small numbers of members? What about galaxy population?

A lot of work… a lot of fun!

THAT’S ALL FOLKS!



Thank you!